Mcl-1 PROMOTES NEURAL PRECURSOR CELL CYCLE EXIT AND DIFFERENTIATION IN THE MOUSE EMBRYONIC BRAIN

S.M. MAHMUDUL HASAN

Mcl-1 promotes Neural Precursor Cell Cycle Exit and Differentiation in the Mouse Embryonic Brain

By

S. M. Mahmudul Hasan

A thesis submitted to the School of Graduate Studies in partial fulfillment of the requirements for a degree of Master of Science (Medicine)

Faculty of Medicine (Neuroscience)
Memorial University of Newfoundland

July 2011

Acknowledgements

I would like to express my gratitude and thank my supervisor, Dr. Jacqueline Vanderluit, for providing me with all the support and best guidance that a student can ask for.

I would also like to thank the members of my lab for their support and encouragement throughout my program.

In addition, I would like to thank my supervisory committee, Dr. Karen Mearow and Dr. Michiru Hirasawa, for providing me with the best advice throughout my program.

Abstract

Neural precursor cell (NPC) proliferation and apoptosis are key regulatory aspects of mammalian nervous system development. Although recent studies suggested these two processes to be interrelated, the molecular mechanisms behind this remain undefined. Here I show that myeloid cell leukemia-1 (Mcl-1), a Bcl-2 family member that is essential for the survival of NPCs also reduces NPC proliferation and promotes their terminal mitosis. I found that within 48 hours of *in utero* electroporating Mcl-1 in E13.5 mouse embryonic brains, the majority of NPCs transfected with Mcl-1 have migrated into the post mitotic cortical plate, whereas control transfected NPCs are still within the proliferating ventricular/subventricular zones. Analysis of proliferation by proliferating cell nuclear antigen (PCNA) immunohistochemistry revealed a 2-fold reduction in proliferating NPCs in the Mcl-1 treated brains. Immunohistochemistry for Tbr1, a marker for newborn neurons, showed a 50% increase in differentiated neurons in Mcl-1 treated brains. BrdU birthdating demonstrated that Mcl-1 overexpression results in a greater cohort of newborn neurons. Furthermore, Mcl-1 transfected NPCs gave rise to neurons in the deeper layers of the cortex than control transfected NPCs confirming an earlier birthdate. Similarly, transfection of Mcl-1 in NPCs *in vitro* promotes cell cycle exit. I showed that Mcl-1 interacts with key cell cycle regulators in NPCs, namely PCNA and Cdk1/Cyclin B1 complex. In addition, I found an increase in Cdk inhibitor $p27^{Kip1}$ protein, a key promoter of cell cycle exit with Mcl-1 overexpression and a concomitant decrease in $p27^{Kip1}$ in Mcl-1 conditional knockout NPCs, suggesting that Mcl-1 may modulate $p27^{Kip1}$ protein to promote NPC differentiation. Finally I showed that $p27^{Kip1}$ is required for Mcl-1 mediated NPC cell cycle exit, suggesting that Mcl-1 regulates NPC cell cycle through $p27^{Kip1}$ activity. In summary, these results identify a novel function for Mcl-1 in promoting terminal mitosis of NPCs by influencing the cell cycle regulatory machinery.

Table of Contents

List of Tables

List of Figures

Chapter 1

Introduction

1.1 Development of the Mammalian Cortex

During embryonic development, neural stem cells (NSCs) give rise to all the neurons and macroglial cells of the mammalian central nervous system (CNS). The differentiated and functionally specialized cells are derived either directly from the stem cells or indirectly via fate-restricted progenitors. Stem cells are defined by their self-renewal capability, ideally for an unlimited number of cell divisions, and multipotency, the ability to give rise to numerous types of differentiated cells (Reynolds and Weiss, 1992). NSCs and the fate-restricted progenitors are collectively called neural precursor cells (NPCs). In the mouse brain, corticogenesis occurs between embryonic days 11-17 (E11-17), when NPCs generate the neurons to form the distinct cortical layers (Takahashi et al., 1996). Initially, NPCs must expand their pool before a proportion of them commit to a specific lineage and differentiate (Noctor et al., 2004, Huttner and Kosodo, 2005). As a result, a balance between proliferation and commitment to a specific lineage regulates the NPC population. Therefore, one of the critical aspects of mammalian brain development is the regulation of NPC cell cycle.

1.1.1 Neuroepithelial Cells

Development of the CNS begins with the formation of the neural tube. The neural tube is formed with the folding of a sheet of neuroepithelial cells, derived from the ectoderm germ layer. Neuroepithelial cells are the primitive neural stem cells, lining the neural tube lumen forming the ventricular zone (Merkle and Alvarez-Buylla, 2006). The neuroepithelial cells are elongated and in contact with both the apical (ventricular) and basal (pial) surfaces (Figure 1.1A). Although the cells divide at the ventricular zone (VZ), they pull the nuclei to the pial surface during interphase. This interkinetic nuclear movement makes the neuroepithelium look 'pseudostratified' or layered (Huttner and Kosodo, 2005, Zhong and Chia, 2008). Before the onset of neurogenesis in mice, the neuroepithelial cells divide symmetrically. This type of cell division generates 2 identical daughter stem cells (Figure 1.1B) and expands the neural stem cell pool (Haubensak et al., 2004, Gotz and Huttner, 2005).

1.1.2 Radial Glial Cells

With the onset of neurogenesis from E11, the neuroepithelial cells switch to asymmetric divisions and generate radial glial cells, which exhibit both residual neuroepithelial and glial properties (Haubensak et al., 2004, Gotz and Huttner, 2005, Tarui et al., 2005). Like neuroepithelial cells, radial glial cells divide in the VZ and maintain contact with the pial surface via a radially projecting basal process (Figure 1.1A). The radial glial cells are the principal progenitors of the embryonic brain and successively replace the neuroepithelial cells. Thus, most of the neurons are generated either directly from radial glial cells or through intermediate progenitors (Anthony et al., 2004, Gotz and Barde, 2005) (Figure 1.1B). Radial glial cells maintain some neuroepithelial

cell properties including interkinetic nuclear migration and expression of the intermediate-filament Nestin (Hartfuss et al., 2001). In addition, they also exhibit several glial characteristics including the astrocyte specific glutamate transporter (GLAST), the Ca^{2+}- binding protein S100β, glial fibrillary acidic protein (GFAP), vimentin and brain-lipid-binding protein (BLBP) (Campbell and Gotz, 2002, Gotz, 2003, Kriegstein and Gotz, 2003).

Figure 1.1: Neurogenesis in the developing cortex

A – An illustration of the developmental changes occurring during corticogenesis between E10-18 (from left to right). Transition of neuroepithelial cells (NEPs) to radial glia occurs after E10/11. The nuclei of neuroepithelial cells and radial glia cells remain at the ventricular zone (VZ) while the basal progenitors occupy the sub-ventricular zone (SVZ). Differentiated neurons make up the cortical plate (CP) following neurogenesis, starting after E11 (Malatesta et al., 2008).

B – The lineage trees show the generation of neurons (N) from neuroepithelial cells (NE) via the stem cell population - radial glial cells (RG), and from the progenitor population that is the basal progenitors (BP) (Gotz and Huttner, 2005).

A

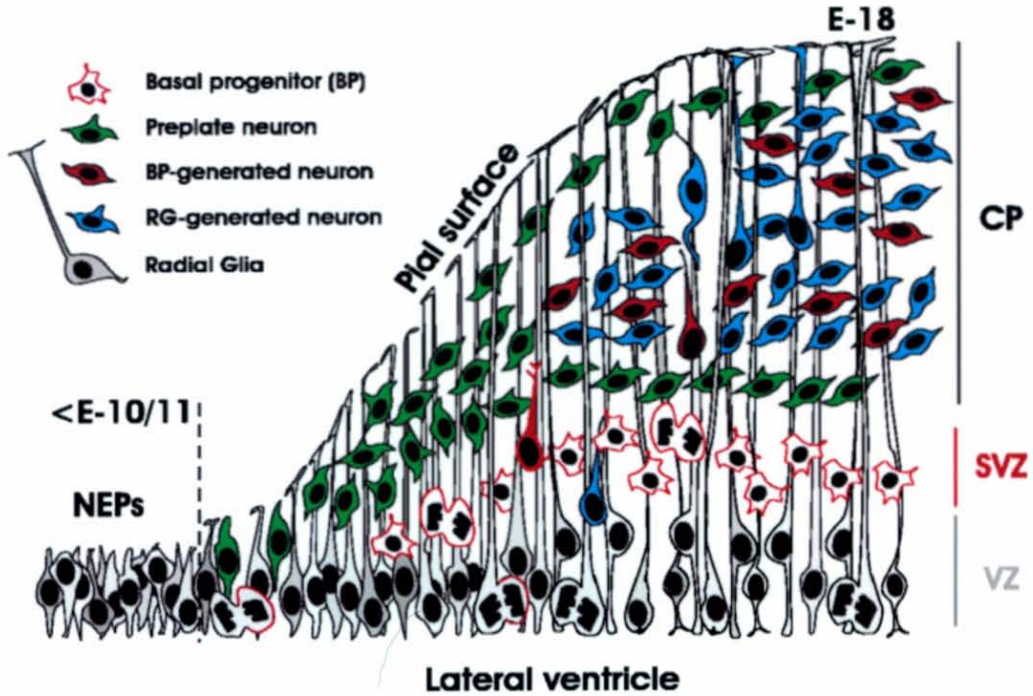
E-18
Basal progenitor (BP)
Preplate neuron
BP-generated neuron
RG-generated neuron
Radial Glia
Pial surface
CP
<E-10/11
NEPs
SVZ
VZ
Lateral ventricle

B

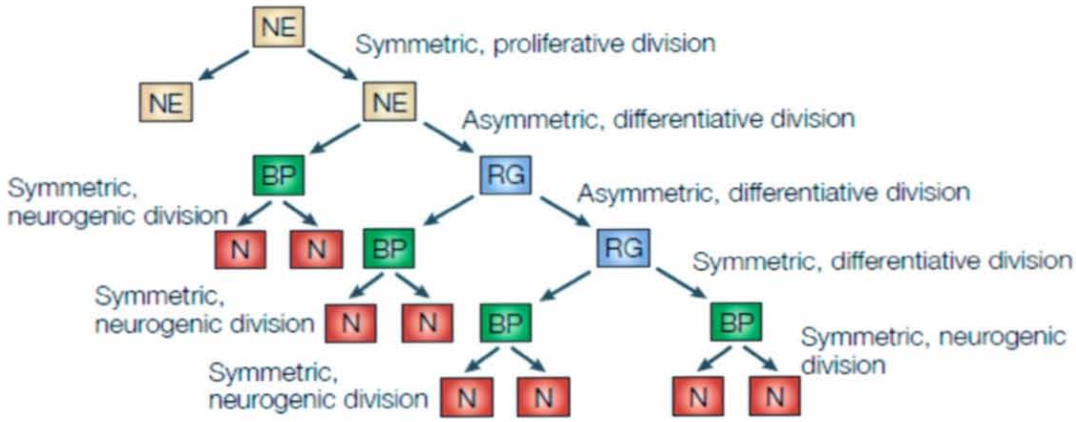
NE
Symmetric, proliferative division
NE
NE
Asymmetric, differentiative division
BP
RG
Symmetric,
neurogenic division
Asymmetric, differentiative division
N
N
BP
RG
Symmetric, differentiative division
Symmetric,
neurogenic division
N
N
BP
BP
Symmetric, neurogenic
division
Symmetric,
neurogenic division
N
N
N
N

1.1.3 Basal Progenitors

During mid-neurogenesis (E13-14), another neuronal progenitor population appears, the basal progenitors or intermediate progenitors. Basal progenitors develop from the divisions of both neuroepithelial cells and the radial glial cells. During later stages of neurogenesis, basal progenitors form the subventricular zone (SVZ), which is a mitotic cell layer basal to the ventricular zone (Haubensak et al., 2004, Miyata et al., 2004, Noctor et al., 2004). Characteristic markers for basal progenitors include transcription factors TBR2, CUX1 and CUX2 (Nieto et al., 2004, Englund et al., 2005).

Basal progenitors contribute to neurogenesis by undergoing symmetric cell divisions and generate two neuronal daughter cells (Figure 1.1A). Therefore, basal progenitors amplify the number of cells produced by a previous progenitor cell division and are an important determinant of brain size (Haubensak et al., 2004, Noctor et al., 2004, Martinez-Cerdeno et al., 2006).

The different stages of neurogenesis can be distinguished by the sequential expression of specific transcription factors (Figure 1.2). NPCs at the VZ express Pax6 and divide to generate the intermediate progenitor cells (IPCs), which migrate to the SVZ and express Tbr2. The IPCs give rise to the NeuroD^{+} committed neuroblasts. Finally, differentiated neurons are generated from neuroblasts and they express Tbr1. Tbr1^{+} neurons migrate to the cortical plate, and so expression of Tbr1 confirms the completion of neurogenesis (Takahashi and Liu, 2006).

Figure 1.2: The changes in transcription factor expression during neurogenic progression.

A –Illustration of a ventricular zone (VZ) NPC (radial glia) progressing to a differentiated neuron in the cortical plate (CP), via basal/intermediate progenitors (IPC) located in the subventricular zone (SVZ). The sequential expression of the specific transcription factors (TFs; top row) and different phases of the cell cycle for radial glia and IPCs (second row from bottom) are also shown.

B – Immunohistochemistry on E14.5 mouse brain further demonstrates the sequential expression of the transcription factors during neurogenic progression of NPCs (Hevner et al., 2006).

(IZ – intermediate zone)

1.2 Organizational Development of the Cortical Layers

During corticogenesis (E11-E19) in mice, the NPCs generate neurons to form the 6-layered cortex (Dehay and Kennedy, 2007). The first neurons form the transient pre-plate, which is then split by later-born neurons to form the superficial marginal zone and deeper sub-plate. The cortical plate (CP) develops between these two layers, and eventually gives rise to the multi-layered neocortex (Figure 1.3) (Molyneaux et al., 2007). The organizational development of the cortical layers is largely regulated by Cajal-Retzius cells, early-born neurons of the marginal zone that express Reelin (Alcantara et al., 1998). Reelin is a large extracellular glycoprotein that plays a role in cell migration and process outgrowth. Mutations of the reelin gene severely disrupt the normal pattern of cortical lamination, resulting in an inverted order of cortical layers II-VI (D'Arcangelo et al., 1995, Hirotsune et al., 1995). The positioning of Cajal-Retzius cells is regulated by the radial glial cells (Kwon et al., 2011).

Cortical plate development is regulated in such a way that the later born neurons that arrive at the cortical plate migrate past the earlier born neurons. This results in the formation of the deeper layers first, followed by the formation of the more superficial layers. The inside-out pattern of corticogenesis results in neurons within a given layer being born at the same time and sharing common functional properties and connectivity (Rakic, 1988, McConnell, 1995). Neurons in the different layers of the post-natal cortex can be distinguished by the expression of specific transcription factors. For example, cut-like transcription factors (Cux1 and Cux2) are expressed in neurons in Layers II-IV and the zinc-finger transcription factors (Fezf2 and Ctip2) are expressed in neurons in deeper Layers V-VI (Figure 1.3) (Leone et al., 2008).

Figure 1.3: The "inside-out" development of the cortex and gene expression patterns during and after corticogenesis.

A – A representation of the development of the mouse neocortex (Ncx) during corticogenesis as shown by the coronal section through the mouse brain at E10.5 (top panel). The embryonic time-point scale shows the sequential development of different layers (bottom panel) (Molyneaux et al., 2007). The multilayered cortex develops in a way that later born neurons arriving at the cortical plate migrate past the earlier born neurons.

B – Expression patterns of different transcription factors during mid-corticogenesis (embryonic: left panel) and after birth (right panel). These markers can be used to identify specific cortical layers in the post-natal brain (Leone et al., 2008).

(CH, cortical hem; IZ, intermediate zone; LGE, lateral ganglionic eminence; MGE, medial ganglionic eminence; SVZ, subventricular zone; VZ, ventricular zone; PP, preplate; MZ, marginal zone; SP, subplate; CP, cortical plate; WM, white matter; I-VI, the distinct cortical layers I-VI)

A

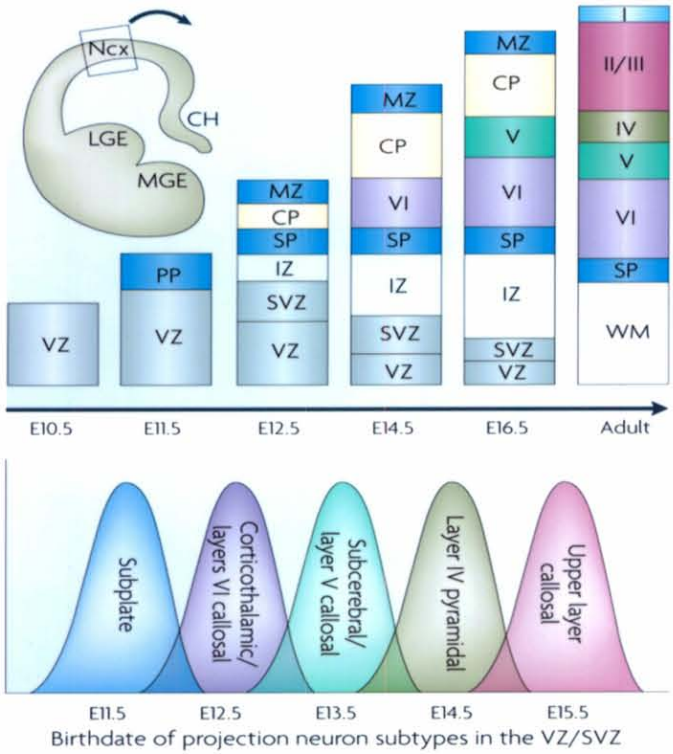

Birthdate of projection neuron subtypes in the VZ/SVZ

B

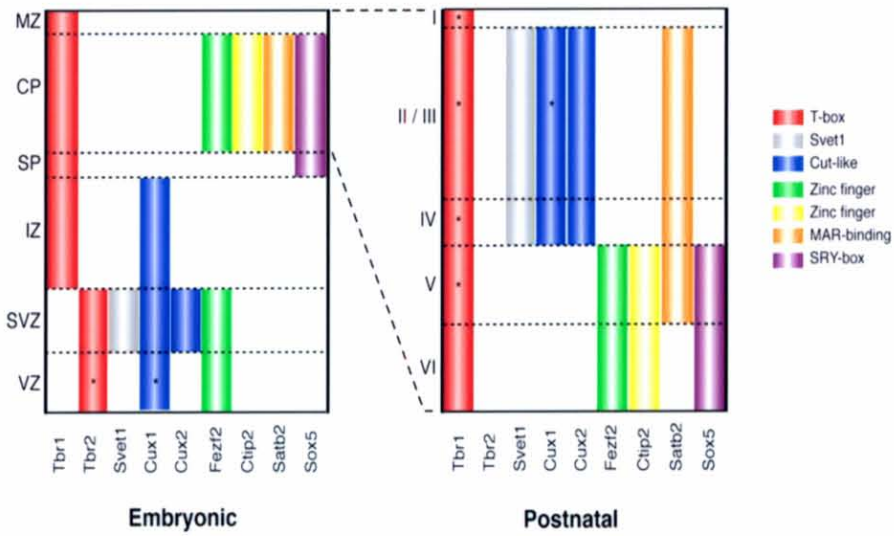

1.3 NPC Proliferation and Differentiation

To form a mature nervous system consisting of the vast number of neurons and glial cells, NPCs must be regulated in a balance between proliferation and their commitment to a specific lineage. This balance is largely controlled by the cell cycle regulatory molecules, which cue the cell to either proliferate or to differentiate with subsequent maturation.

1.3.1 Regulation of NPC Cell Cycle

Like all somatic cells, signaling pathways that direct entry, progression into and exit from the cell cycle regulates NPC proliferation. The cell cycle of an actively dividing cell is composed of 4 phases: synthesis (S), mitosis (M) and two gap (G1 and G2) phases (Figure 1.4A). The S phase is responsible for replication of genomic DNA and the M phase is dedicated for physical division of cellular and genomic contents into two individual cells. The first gap phase (G1) occurs between the end of M phase and the beginning of S phase. G1 phase consists of a critical restriction point (R), when the cell either commits to the next round of cell division or exits the cell cycle to enter G0 phase. The second gap phase (G2), between the end of S phase and beginning of M phase, is dedicated to repair any errors in DNA replication and prepares the cell for mitosis (Figure 1.4A) (Pardee, 1989, Nurse, 1994).

During cortical neurogenesis, the G1 restriction point (R) has been identified as the critical cell cycle regulation point. Each successive cycles of NPC and their restricted progenitor result in a greater proportion of post-mitotic cells that exit the cell cycle at R (Caviness et al., 1999). This restriction point R is regulated by the Retinoblastoma gene family and E2F transcription factors.

1.3.2 Retinoblastoma gene and E2F transcription factors

The retinoblastoma gene (Rb) was the first tumour suppressor to be identified for its mutations leading to pediatric eye tumour development (Fung et al., 1987, Lee et al., 1987). Rb family proteins include pRb, p130 and p107, all sharing the structural homology of the functional A/B pocket (Classon and Dyson, 2001). This functional domain can interact with transcriptional regulators like the E2F transcription factors, a family of proteins that share a related DNA-binding domain. E2F transcription factors bind to sets of target promoters and activate or repress transcription. Therefore, Rb/E2F activity plays a pivotal role in regulating cell cycle progression by controlling transcription of target genes (Polager and Ginsberg, 2008).

During the G1 phase of the cell cycle, Cyclin dependent kinase and Cyclin activity hyperphosphorylates Rb (Figure 1.4). Once hyperphosphorylated, Rb releases the E2F transcription factors (E2F-1, 2, 3), which are the activators of gene transcription that is essential for the G1 to S phase transition and commitment to mitosis (Dyson, 1998, Nevins, 1998). Overexpression of Rb causes cells to remain in quiescence or prolonged G1 phase, whereas overexpression of E2Fs induces quiescent immortalized cells to re-enter the cell cycle (Polager and Ginsberg, 2008).

The function of Rb and consequently E2Fs is critical for neurogenesis and the development of the CNS. Germline knockout of Rb results in embryonic lethality at E15.5 due to hematopoietic and neurological defects. Conditionally knocking out Rb results in ectopic mitosis within the developing brain and although NPCs commit to a differentiated fate, they fail to exit the cell cycle (Ferguson et al., 2002). This is a result of enhanced E2F-1 and E2F-3 activity that delays the terminal mitosis of NPCs differentiating in absence of Rb (Callaghan et al., 1999). Rb family member, p107, has also been identified to regulate the NPC pool. Although p107 null mice

exhibit increased proliferating progenitor cells, the p107-/- progenitors show impaired neuronal commitment (Callaghan et al., 1999, Vanderluit et al., 2004, Vanderluit et al., 2007). Therefore, Rb and related proteins and their E2F targets regulate the NPC cell cycle progression and cell cycle exit.

1.3.3 Cyclin-dependent kinases and Cyclins

Cyclin-dependent kinases (Cdks) regulate the progression through each of the phases of the cell cycle. Cdks are activated by phosphorylation/dephosphorylation events as they bind to specific Cyclin partners, their regulatory subunits. Distinct Cyclins are synthesized and then destroyed at specific phases of the cell cycle, adding another regulatory step for Cdk-Cyclin activity (Nigg, 1995). There are 4 Cdks (Cdk1, Cdk2, Cdk4 and Cdk6) and 10 Cyclins that belong to 4 different classes (Cyclin A, Cyclin B, Cyclin D and Cyclin E type), and are responsible for cell cycle progression (Malumbres and Barbacid, 2009).

The initiation and progression through G1 is mediated by activation of multiple signaling pathways that converge on the transcription of immediate early genes, D-type Cyclins, and their assembly with Cdk4/6 kinases (Sherr, 1995, Roussel, 1998). Once activated, Cyclin D-Cdk4/6 complexes preferentially phosphorylate pRb and pRb-related proteins p107 and p130 (Sherr, 1994, Weinberg, 1995). This is followed by additional phosphorylation by the Cyclin E-Cdk2 and progression into the cell cycle (Ohtsubo et al., 1995) (Figure 1.4B). During S and G2 phase, continuous Cyclin A-Cdk2 activity is required but the transition to mitosis requires Cyclin B-Cdk1 activation by the phosphatase cdc25c (King et al., 1994, Nurse, 1994) (Figure 1.4A). Activity of all Cdks are regulated at multiple levels including the abundance of Cyclins,

activating or deactivating phosphorylation of Cdk subunits and the abundance of endogenous Cdk inhibitor proteins (Figure 1.3) (Cunningham and Roussel, 2001, Musgrove et al., 2004).

Recently, the idea that activity of all Cdks is required for progressing through the mammalian cell cycle has been challenged. Even in the absence of all interphase Cdks (Cdk2, Cdk3, Cdk4 and Cdk6), the mouse embryo can undergo organogenesis with continued development until midgestation. Under these circumstances, Cdk1 binds to all Cyclins and phosphorylates pRb, resulting in the expression of genes that are regulated by E2F transcription factors (Santamaria et al., 2007). Cdk1 can also bring cells out of quiescence in the absence of interphase Cdks by interacting with Cyclin-D and/or Cyclin-E to phosphorylate Rb (Martin et al., 2005). However, Cdk1 knockout mouse embryos fail to develop to the morula or blastocyst stage, suggesting that other Cdks do not have the same compensatory capacity as Cdk1 (Santamaria et al., 2007).

1.3.4 Cyclin-dependent kinase inhibitors

Cyclin-dependent kinase inhibitor proteins are important in regulating Cdk activity, and hence the progression of cell cycle or cell quiescence. Two families of Cdk inhibitors promote cell cycle exit by blocking the activity of Cdk-Cyclin complexes: the Cip/Kip family, including $p21^{Cip1}$, $p27^{Kip1}$, and $p57^{Kip2}$, and the INK4 family, including $p15^{Ink4b}$, $p16^{Ink4a}$, $p18^{Ink4c}$, and $p19^{Ink4d}$ (Elledge and Harper, 1994).

Although the Cip/Kip family of inhibitors can interact with all Cdk-Cyclin complexes, $p27^{Kip1}$ is the main Cip/Kip inhibitor in NPCs during development. The other family members, $p21^{Cip1}$ and $p57^{Kip2}$, are only expressed in post mitotic cells within the cortical plate (Nguyen et al., 2006). $P27^{Kip1}$ promotes cell cycle arrest of neural progenitor cells during embryogenesis (Fero et al., 1996, Kiyokawa et al., 1996, Nakayama et al., 1996, Carruthers et al., 2003), reduces

proliferation of transit amplifying progenitors in the adult subventricular zone (Doetsch et al., 2002), and, together with $p19^{Ink4d}$, maintains differentiated neurons in a non-mitotic state (Zindy et al., 1999). The $p27^{Kip1}$-null mice exhibit multi-organ hyperplasia from enhanced cell proliferation. In addition, the $p27^{Kip1}$-null mutants demonstrate a decrease in neuronal production during mid-corticogenesis and an increase in production of late-born neurons. This delay in cell cycle exit results in an enlargement of upper cortical layers (Goto et al., 2004). Similarly, overexpressing $p27^{Kip1}$ in cortical progenitors promotes premature cell cycle exit and results in a reduction of upper layer neurons (Tarui et al., 2005).

In addition to promoting cell cycle exit, Cdk inhibitor $p27^{Kip1}$ also promotes differentiation and radial migration of cortical projection neurons. The N-terminus of $p27^{Kip1}$ is involved in stabilizing Neurogenin-2 protein, a proneural basic helix-loop-helix (bHLH) factor, which specifies cortical progenitors to a neuronal fate. The C-terminus half of $p27^{Kip1}$ inactivates GTPase RhoA, a modulator of intracellular actin dynamics and influences cortical neuronal migration (Nguyen et al., 2006). Therefore, $p27^{Kip1}$ plays a crucial role in neuronal development by promoting cell cycle exit of NPCs, as well as their differentiation and migration.

The $p27^{Kip1}$ protein is regulated via priming phosphorylation, ubiquitination followed by proteasomal degradation (Pagano et al., 1995, Loda et al., 1997). Cdk-mediated phosphorylation on T187 of $p27^{Kip1}$ is required for ubiquitination. This represents a feedback mechanism by which Cdks can regulate $p27^{Kip1}$ turnover. Phosphorylation of $p27^{Kip1}$ on T187 by Cdk-cyclin complex requires formation of a stable trimeric complex. However, although Cdk1-Cyclin B1 phosphorylates $p27^{Kip1}$ on T187, it fails to form a stable complex with $p27^{Kip1}$ and thus cannot direct its ubiquitination by E3 ligase (Montagnoli et al., 1999). Whether the phosphorylation of $p27^{Kip1}$ on T187 by Cdk1-Cyclin B1 affects its functional role is still unknown.

Apart from the T187 residue, regulatory phosphorylation of $p27^{Kip1}$ protein also occurs on S10. Arginine directed serine/threonine kinases like Mirk/dyrk1B phosphorylates $p27^{Kip1}$ on S10. This stabilizes $p27^{Kip1}$ protein and enhances its functional properties as a Cdk inhibitor, binding to Cdk2 (Deng et al., 2004). Interestingly in neural stem cells, Cdk5 can phosphorylate $p27^{Kip1}$ on both S10 and T187. Phosphorylation on both sites promotes neuronal differentiation from cell cycle arrest followed by neurite outgrowth and migration (Zheng et al., 2010). Therefore, phosphorylation of $p27^{Kip1}$ is a critical regulatory step in promoting cell cycle exit of NPCs and their differentiation.

Figure 1.4: Cell cycle regulation by Cdks (Cyclin dependent kinases), cyclins, Cdk inhibitors and the Rb/E2F pathway.

A – Schematic of the eukaryotic cell cycle showing the different phases – G1, S, G2, M and the critical restriction point R. The specific Cdk-cyclin complexes responsible for progression through each phase are shown with their INK or KIP/CIP inhibitors (Adapted from (Dehay and Kennedy, 2007).

B – To progress through the G1 restriction point, G1 Cdk-cyclin complexes hyperphosphorylate Rb freeing E2F transcription factors. Free E2Fs promote transcription of target genes and progression into the S phase.

A

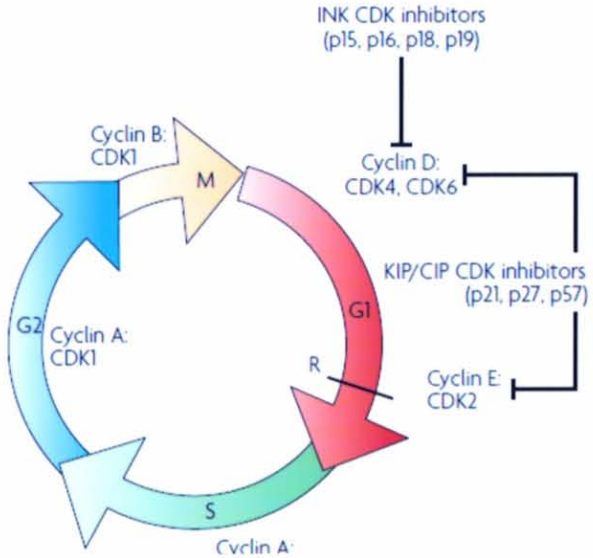
INK CDK inhibitors
(p15, p16, p18, p19)
Cyclin B:
CDK1
M
Cyclin D:
CDK4, CDK6
KIP/CIP CDK inhibitors
(p21, p27, p57)
G1
G2
Cyclin A:
CDK1
R
Cyclin E:
CDK2
S
Cyclin A:

B

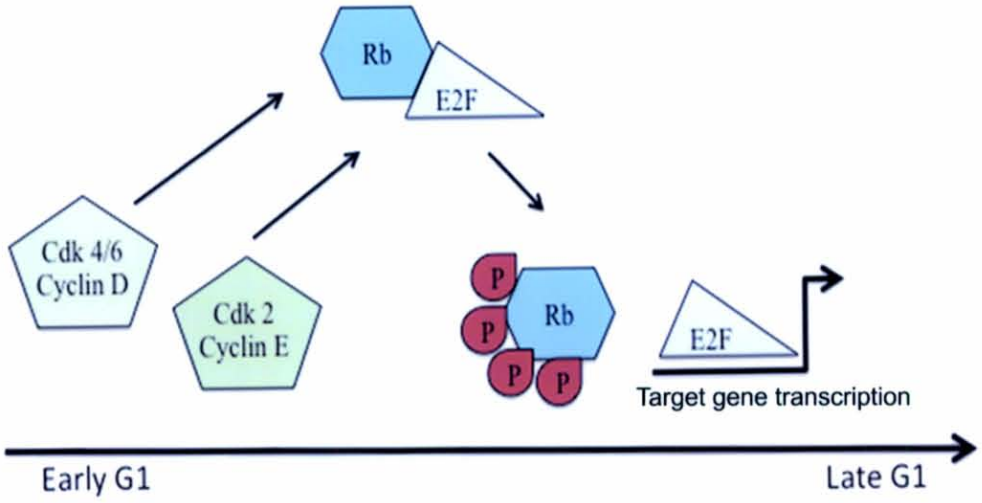
Rb
E2F
Cdk 4/6
Cyclin D
Cdk 2
Cyclin E
P
P
P
P
Rb
E2F
Target gene transcription
Early G1
Late G1

1.4 Survival of Neural Precursor Cells

The survival of NPCs is important to ensure the appropriate number of neurons within the different layers of the cortex. During neurogenesis, NPCs and neurons are made in excess. This ensures that if a portion of the cells exhibit defects during cell division, differentiation or maturation, they can be eliminated. Cells exhibiting such defects and the excess cells are eliminated by apoptosis (Nicholson et al., 1995, Haydar et al., 1999). At E10 only rare apoptotic cells are observed when the NPCs are undergoing symmetric divisions to expand their pool. However, by late-neurogenesis at E18, 50-70% of NPCs are dying (Blaschke et al., 1996). This massive cell death is required to regulate the NPC population size and eventually the brain size and shape. After neurogenesis is complete, there is a second wave of apoptosis among differentiated neurons. This eliminates neurons that have failed to form connections with other cells and so are not parts of the functional circuitry (de la Rosa and de Pablo, 2000, Blomgren et al., 2007).

Studies on pro-apoptotic proteins and aspartate-specific cysteine proteases (caspases) have provided insights on NPC survival. Specially, studies on Caspase-3 deficient mice revealed hyperplasia of the NPC population during CNS development. This demonstrated that the programmed cell death of NPCs and neurons during development is apoptotic (Nicholson et al., 1995, Haydar et al., 1999, Roth et al., 2000). Apoptosis is an energy dependent form of cell death that is characterized by DNA fragmentation, nuclear condensation and membrane changes without induction of an immune response (Kerr et al., 1972). There are two main families of proteins that regulate apoptosis: the Caspase family and the B-cell lymphoma (Bcl-2) family (Youle and Strasser, 2008).

1.4.1 Caspase family

Caspases are classified as either initiator caspases or executioner caspases. Initiator caspases have a caspase recruitment domain (CARD) that allows them to interact with other apoptosis initiating molecules like apoptotic protease activating factor-1 (Apaf-1), which cleaves and activates executioner caspases. Once activated, executioner caspases cleave cellular proteins resulting in the physiological characteristics of apoptosis, including plasma membrane blebbing and nuclear condensation (Fan et al., 2005, Wang et al., 2005).

Caspase family members are involved in developmental apoptosis within the mammalian cortex. Caspase-3 and caspase-9 null-mice exhibit hypercellularity due to impaired cell death. This results in an expanded cortex and ultimately lethality during the perinatal period (Kuida et al., 1998, Haydar et al., 1999).

1.4.2 Bcl-2 family

The Bcl-2 family of proteins is characterized by the presence of 1-4 BH domains. It is divided into 3 subtypes based on the functional homology of the Bcl-2 family members. The anti-apoptotic Bcl-2 proteins are Bcl-2, Bcl-xL, Bcl-W, Mcl-1 and A1, and they inhibit the activity of pro-apoptotic Bcl-2 proteins. Bcl-2, Bcl-xL and Bcl-W have all four BH domains, whereas Mcl-1 does not have a BH4 domain and A1 lacks both BH3 and BH4 domains (Youle and Strasser, 2008). These pro-apoptotic proteins are either effector proteins containing BH-1 to BH-3 domains, including Bak and Bax, or the BH3 domain only. The BH3 only pro-apoptotic proteins activate the cell intrinsic apoptotic pathway and include Puma, Noxa, Bim, Bad, Bid, Hrk and Bmf (Figure 1.5) (Chipuk and Green, 2008, Youle and Strasser, 2008). Collectively, the BH3

only proteins facilitate the oligomerization of Bak and Bax, which leads to mitochondrial membrane permeabilization and ultimately apoptosis.

The expression of anti-apoptotic Bcl-2 proteins varies throughout development. Within the developing CNS, Bcl-2 expression peaks between E11-15 and then declines to an undetectable level by the time of birth (Krajewska et al., 2002). Although Bcl-2 targeted deletion in mice does not affect neuronal development, postnatally it results in a significant loss of sympathetic, motor, and sensory neurons (Michaelidis et al., 1996). Bcl-xL expression is first seen in post-mitotic neurons after E10.5 (Krajewska et al., 2002). Conditional deletion of Bcl-xL in catecholaminergic neurons results in viable mice with a reduction in the catecholaminergic neuronal population by one-third (Savitt et al., 2005).

In comparison, germline knockout of anti-apoptotic Mcl-1 results in peri-implantation lethality due to defects in differentiation of the trophectoderm (Rinkenberger et al., 2000). Conditional knockout (CKO) of Mcl-1 within the NPC population results in widespread apoptosis and embryonic lethality at E15. Mcl-1 CKO embryos show apoptosis among Nestin expressing precursor cells, Doublecortin expressing migrating precursor cells and βIII tubulin (Tuj1) expressing newborn neurons (Arbour et al., 2008). This demonstrates that Mcl-1 is required for the survival of both proliferating and differentiating NPCs. Additionally, unpublished data from our lab has identified Mcl-1 as a survival factor of embryonic neural stem cells (NSCs). To assess self-renewal of embryonic NSCs, we performed a secondary neurosphere assay (Vanderluit et al., 2004) and demonstrated that Mcl-1 CKO results in a 4-fold reduction in secondary neurospheres when compared to wildtype controls. Therefore, Mcl-1 is a critical survival factor of both NSCs and NPCs. This is unique to Mcl-1, since all other Bcl-2 pro-survival proteins expressed in the CNS, like Bcl-2 and Bcl-xL, are required for the survival of post-mitotic neurons.

Figure 1.5: Bcl-2 family of proteins

The Bcl-2 family is divided into the anti-apoptotic, pro-apoptotic and BH3-only pro-apoptotic subfamily. The BH domains are illustrated as BH1, BH2, BH3 and BH4, while the transmembrane domain is denoted as TM. The PEST sequence is also shown on Mcl-1 (Adapted from (Youle and Strasser, 2008).

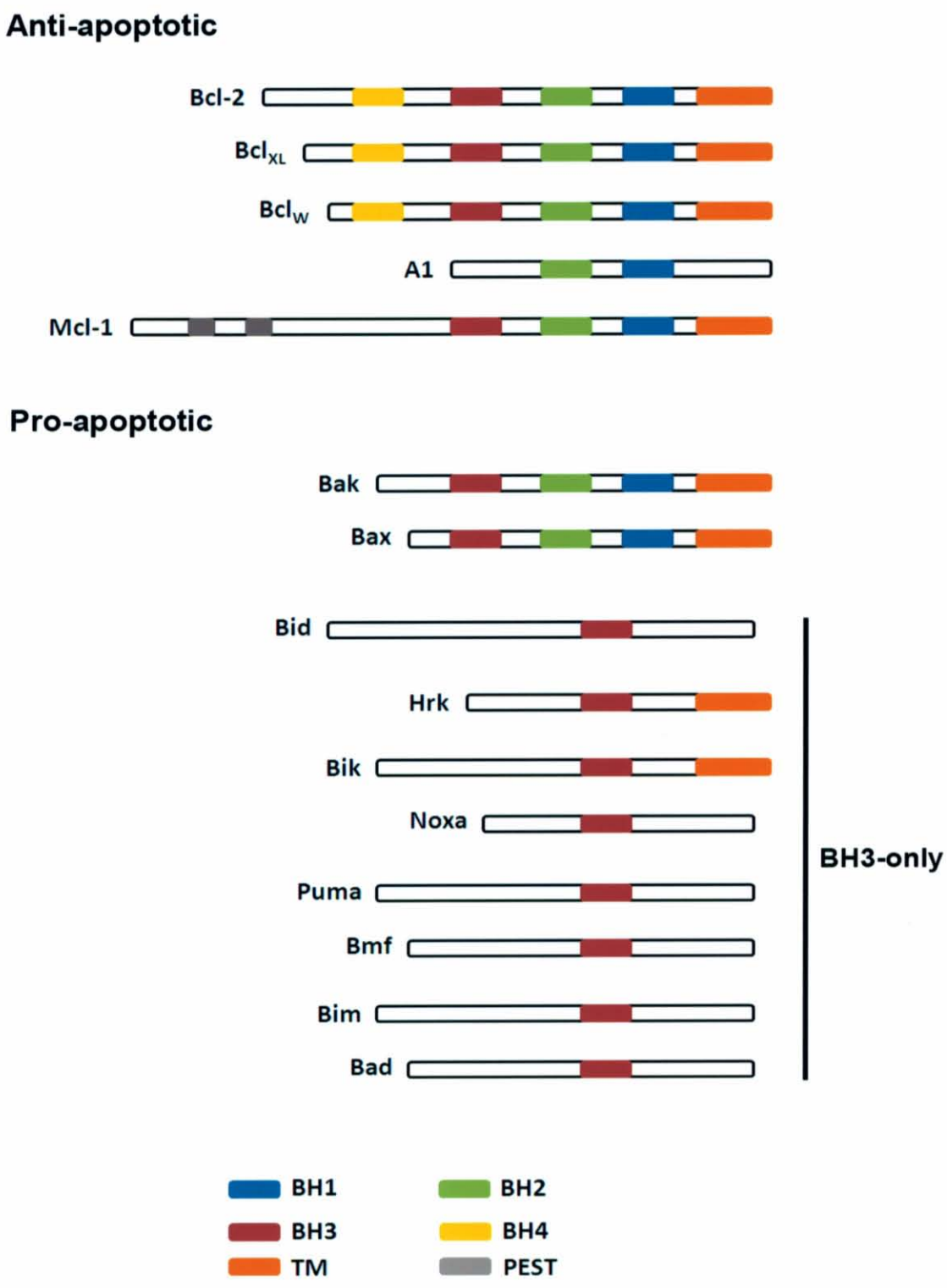
Anti-apoptotic
Bcl-2
Bcl$_{XL}$
Bcl$_{W}$
A1
Mcl-1
Pro-apoptotic
Bak
Bax
Bid
Hrk
Bik
Noxa
Puma
Bmf
Bim
Bad
BH3-only
BH1
BH2
BH3
BH4
TM
PEST

1.5 Bcl-2 Family and the Cell Cycle

Besides apoptosis, some members of the Bcl-2 family of proteins regulate cell cycle progression (Table 1.1). Forced expression of some pro-apoptotic Bcl-2 proteins, in the presence of apoptosis inhibitors, promote cell cycle progression and are proliferative. In contrast, forced expression of pro-survival Bcl-2 and Bcl-xL proteins arrest cell cycle progression and are anti-proliferative (Zinkel et al., 2006).

Overexpression of Bcl-2 protein slows cell cycle entry in NIH 3T3 cell lines by promoting expression of the Cdk inhibitor $p27^{Kip1}$ and pRb relative p130. Increase in p130 results in the formation of repressive p130-E2F4 complexes and delay in the expression of E2F1, which is required for the cell cycle progression (Vairo et al., 2000). Elevation of $p27^{Kip1}$ protein also occurs with Bcl-xL overexpression and induces delayed cell cycle progression. The elevated $p27^{Kip1}$ protein delays activation of Cdk2 and Cdk4 during progression into S-phase (Greider et al., 2002). Therefore, forced expression of some anti-apoptotic Bcl-2 members in cell lines confers anti-proliferative effects.

However, the anti-proliferative effects of Bcl-xL can be reversed by the pro-apoptotic Bcl-2 member Bad. Induced Bad expression in fibroblasts results in continued proliferation and sustained Cdk2-cyclin E activity. Bad also forms heterodimers with Bcl-xL to overcome the G0/G1 checkpoint and continue cell cycle progression (Chattopadhyay et al., 2001).

Overexpression of some other pro-apoptotic Bcl-2 members in the presence of apoptosis inhibitors also increases proliferation. Transgenic overexpression of Bax-alpha increases the number of proliferating thymocytes, reduces the level of $p27^{Kip1}$ in mature T-cells and promotes rapid progression to S-phase (Brady et al., 1996). Germline knockout of another pro-apoptotic member, Bid, results in impaired hepatic cell proliferation and carcinogenesis, demonstrating its

role in cell cycle regulation (Bai et al., 2005).

It has been demonstrated that the dual roles of some Bcl-2 family members in cell cycle progression and cell survival are functionally separate. Site-specific mutation of a tyrosine residue within the N-terminal BH4 region of Bcl-2 abolishes its function in cell cycle progression but has no effect on cell survival (Huang et al., 1997).

Bcl-2 family	Role in survival or apoptosis	Role in proliferation	Role in cell cycle
Anti-apoptotic			
Bcl-2	° Transgenic overexpression protects neurons from developmental and induced cell death (Allsopp et al., 1993, Martinou et al., 1994, Farlie et al., 1995) ° Bcl-2 -/- post natal apoptosis in sympathetic, sensory and motor neurons (Michaelidis et al., 1996)	° Anti-proliferative (Vairo et al., 2000, Greider et al., 2002)	° Delays myc-induced progression to G1/S (Vairo et al., 2000, Greider et al., 2002) ° Delays G1 progression by altered E2F regulation (Vairo et al., 2000)
Bcl-xL	° Bcl-xL -/- results in widespread apoptosis in hematopoietic cells and immature neurons (Motoyama et al., 1995) ° Bcl-xL overexpression rescues 60% of cholinergic neurons from axotomized cell death (Blomer et al., 1998)	° Anti-proliferative (Greider et al., 2002)	° Delays myc-induced progression to G1/S (Greider et al., 2002)
Mcl-1	° Germline -/- is peri-implantation lethal at E3.5 (Rinkenberger et al., 2000) ° Conditional -/- results in widespread apoptosis in neural precursor cells, migrating neuroblasts and immature neurons (Arbour et al., 2008).	° Anti-proliferative (Fujise et al., 2000, Jamil et al., 2005)	° Slows cell cycle progression at S-phase by interacting with PCNA (Fujise et al., 2000, Jamil et al., 2005) ° Slows cell cycle at G2/M transition by interacting with Cdk1 (Jamil et al., 2005)
Pro-apoptotic			
Bax	° Required for neuronal death during development and under trophic factor deprivation (Deckwerth et al., 1996, Deshmukh and Johnson, 1998, White et al., 1998).	° Promotes proliferation (Brady et al., 1996, Knudson et al., 2001)	° Promotes S-phase entry by reducing $p27^{Kip1}$ expression (Brady et al., 1996, Knudson et al., 2001)
Pro-apoptotic BH3-only			
Bad	° Apoptotic stimuli mediated dephosphorylation initiates downstream apoptotic cascade (Datta et al., 1997, Zhu et al., 2002) ° Overexpression induces death (Orike et al., 2001)	- unknown	° Causes S-phase progression by increasing Cyclin E/Cdk2 activity (Chattopadhyay et al., 2001)
Bid	° No effect on neuronal cell death (Leonard et al., 2001)	° Promotes proliferation (Bai et al., 2005)	° Promotes S-phase progression (Bai et al., 2005)

Table 1.1: Bcl-2 family members that function in cell apoptosis and proliferation (-/- = knockout, E3.5 = embryonic day 3.5)

1.6 Mcl-1 Regulation of Cell Survival

Mcl-1 is an anti-apoptotic member of the Bcl-2 family. Full length Mcl-1 protein contains a transmembrane domain, which localizes it to the outer-mitochondrial membrane, where it interacts with pro-apoptotic Bcl-2 members like Bim, Bmf, Puma, Noxa and Bak to prevent cell apoptosis (Warr and Shore, 2008). Mcl-1 protein also has 3 BH domains and 2 PEST sequences (Kozopas et al., 1993, Youle and Strasser, 2008). PEST sequences are associated with proteins with short half-lives and are absent in other Bcl-2 pro-survival members (Fujise et al., 2000). Alternative splicing of the Mcl-1 mRNA results in a splice variant containing only the BH-3 domain. The shorter Mcl-1 protein is functionally opposite to full length Mcl-1 fragment and promotes cell death (Bingle et al., 2000). Therefore, processing of Mcl-1 mRNA is important in determining its role in cell survival.

Mcl-1 was first discovered as a gene that is upregulated during induced differentiation of human myeloblastic leukemia cells ML-1 (Kozopas et al., 1993). However, studies on Mcl-1 loss-of-function have been restricted since germline knockout of Mcl-1 results in the peri-implantation lethality of mice at E3.5. This lethality is due to defects in differentiation of the trophectoderm (Rinkenberger et al., 2000). It is the most severe phenotype among all of the Bcl-2 anti-apoptotic proteins. Since Mcl-1 germline knockouts are embryonic lethal, our current understanding of the functions of Mcl-1 come from conditional knockout models using the Cre-lox system (Sauer, 1998). Conditional knockout model for Mcl-1 was first generated to assess the function of Mcl-1 in hematopoietic system development (Opferman et al., 2005). It was demonstrated that Mcl-1 is essential for the survival of hematopoietic stem cells and the development and survival of B and T lymphocytes. The subsequent generation of Mcl-1 knockouts in hepatocytes and keratinocytes

resulted in widespread apoptosis within both populations. This identifies the survival role of Mcl-1 in hepatic and epidermal proliferating precursors (Sitailo et al., 2009, Vick et al., 2009). While promoting survival of epidermal keratinocytes, Mcl-1 also induces expression of keratinocyte differentiation markers, indicating that its role may be critical at the time of differentiation (Sitailo et al., 2009).

Conditional knockout of Mcl-1 in the NPC population causes widespread apoptosis in both proliferating and differentiating NPCs. In the absence of Mcl-1, NPCs undergo apoptosis as they migrate away from the ventricular zone and commit to a neuronal fate (Arbour et al., 2008). In fact, Mcl-1 is the only Bcl-2 family member that is required for the survival of embryonic NPCs. Thus, Mcl-1 appears to be a critical regulator during the time of differentiation or cell cycle exit of NPCs.

1.7 Regulation of Mcl-1 Protein

Regulation of Mcl-1 is achieved at multiple levels - transcriptional, post-transcriptional and post-translational (Wang et al., 1999, Bingle et al., 2000, Craig, 2002, Wang et al., 2003). Unlike its other anti-apoptotic Bcl-2 family members, Mcl-1 protein is labile with a short half-life. Depending on the cell type and context, its half-life ranges from minutes to a few hours (Craig, 2002, Cuconati et al., 2003, Adams and Cooper, 2007). Mcl-1 protein is regulated by phosphorylation and ubiquitination followed by proteasomal degradation. Mcl-1 ubiquitin ligase E3 (Mule), an ubiquitin ligase containing a BH-3 domain, interacts with Mcl-1 and ubiquitinates its 5 lysine residues that result in proteasomal degradation (Warr et al., 2005, Zhong et al., 2005). Glycogen synthase kinase 3 (GSK-3) also phosphorylates Mcl-1 and primes it for ubiquitination

by the E3 ligase beta-TrCP, promoting its degradation (Ding et al., 2007). Both ubiquitinating pathways are opposed by the deubiquitinase USPX, which removes the lysine linked polyubiquitin chains and prevents proteasomal degradation of Mcl-1 (Schwickart et al., 2010). Substituting the lysine residues in Mcl-1 with arginine can extend the half-life of the protein (Zhong et al., 2005). This demonstrates that proteasomal degradation is the major regulator of Mcl-1 protein and that prevention of its rapid degradation offers a way to effectively overexpress Mcl-1.

Mcl-1 protein is also regulated throughout the cell cycle and peaks at mitosis. During mitotic arrest, Cdk1–Cyclin B1 phosphorylates Mcl-1 at Ser64 and Thr92. This phosphorylation initiates degradation of Mcl-1 by proteasomal activity of the anaphase-promoting complex/cyclosome (APC/C) E3 ubiquitin ligase (Harley et al., 2010). Thus, phosphorylation of Mcl-1 by Cdk1–Cyclin B1 and its APC/C mediated degradation initiates apoptosis of cells arrested in mitosis.

1.8 Mcl-1 and the Cell Cycle

In vitro, Mcl-1 has been shown to affect cell cycle progression. Forced expression of Mcl-1 in cell lines leads to decreased BrdU (bromodeoxyuridine) intake, a measure of cell proliferation, and a slower doubling rate (Fujise et al., 2000, Jamil et al., 2005). Mcl-1 interacts with PCNA (proliferating cell nuclear antigen), a factor for DNA Polymerase δ activity during DNA replication. This slows cell cycle progression into S-phase in HEK 293T, HeLa and U20S cell lines (Fujise et al., 2000). Furthermore, a proteolytic fragment of Mcl-1 has been demonstrated to bind to Cdk1 resulting in a lower rate of proliferation in a murine myeloid progenitor cell line. Cdk1 regulates progression through G2 and M phases of the cell cycle by binding with Cyclin B

and phosphorylating multiple downstream targets (Jamil et al., 2005). Therefore, Mcl-1 may affect the cell cycle kinetics at different phases and reduce cell proliferation. Recently, conditional knockout of Mcl-1 in hepatocytes resulted increased proliferation and hepatocellular carcinoma development (Weber et al., 2010).

1.9 Rationale and Hypothesis

Neural precursor cell proliferation and apoptosis are crucial regulatory aspects of mammalian nervous system development. Although recent evidence suggests that these two processes are interrelated, the molecular mechanisms behind them are not well established. Mcl-1 is a critical survival factor for both proliferating and differentiating embryonic NPCs (Arbour *at al.* 2008). In addition, recent studies in cell lines show that Mcl-1 can also affect cell cycle kinetics upon forced expression (Fujise *et al* 2000, Jamil *et al.* 2005). However, the role of Mcl-1 in regulating cell cycle progression under physiological *in vivo* conditions has not yet been demonstrated.

Therefore, I put forward the following hypothesis-

Hypothesis:

Mcl-1 regulates cell cycle progression and promotes differentiation of NPCs within the embryonic brain.

Objectives:

The main objectives of this thesis are-

1. To determine whether Mcl-1 regulates embryonic NPC proliferation and differentiation.
2. To determine the mechanism by which Mcl-1 regulates NPC cycle progression.

Chapter 2

Materials & Methods

2.1 Mice

Mice were kept on a 12-hour light/dark cycle and food/water was administered *ad libitum*. All experiments were approved by Memorial University's Animal Care Ethics Committee, adhering to the Guidelines of the Canadian Council on Animal Care.

CD-1 mice were provided from Charles River Laboratories. For breeding, mice were housed in the same cage for up to 3 days and the formation of the plug was checked every 12 hours. For embryonic time points, the time of plug identification was considered to be embryonic day 0.5 (E 0.5) and the male mouse was immediately separated upon detection of the plug. Floxed Mcl-1 (Mcl-$1^{f/f}$) transgenic mice were generated in the laboratory of Dr. S. Korsmeyer (Opferman et al., 2005) and Nestin Cre ($Cre^{+/-}$) transgenic mice were generated in the laboratory of Dr. R. Slack (Berube et al., 2005). Both were maintained on a FVBN background. Mcl-1 conditional knockout (CKO) mice were generated by crossing Nestin Cre transgenic mice with Mcl-1 floxed (Mcl-$1^{f/f}$) adults as described by (Arbour et al., 2008) and illustrated in Figure 2.1. Mcl-1 CKO ($Cre^{+/-}$:Mcl-$1^{f/f}$) mice were compared to littermate controls (Mcl-$1^{+/+}$) for all experiments studying Mcl-1 loss-of-function. The $p27^{Kip1}$ knockout embryos ($p27^{Kip1\ -/-}$) were generated by crossing $p27^{Kip1}$ heterozygous males ($p27^{Kip1\ +/-}$) with $p27^{Kip1}$ heterozygous females ($p27^{Kip1\ +/-}$) (Fero et al., 1996), both maintained on a C57BL/6 background. For loss-of-function studies, $p27^{Kip1}$ knockout embryos ($p27^{Kip1\ -/-}$) were compared to wildtype littermate controls ($p27^{Kip1\ +/+}$).

Figure 2.1: Conditional Mcl-1 Knockout mediated by Cre recombinase.

Mcl-$1^{f/f}$ mouse is crossed with Nestin Cre transgenic mice. The Nestin promoter mediates expression of Cre recombinase and the DNA between the loxP sites is excised. Therefore, Mcl-1 is conditionally knocked out from neural tissue using the neural specific Nestin promoter.

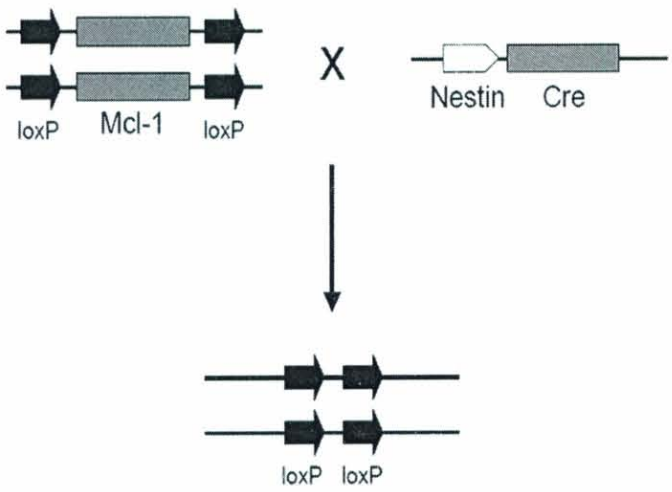
loxP
Mcl-1
loxP
X
Nestin
Cre
loxP
loxP

2.2 Genotyping Mice

To determine the genotype, DNA was isolated from tail clippings of adults and limb buds of embryos at embryonic day 13 (E 13) using the REDExtract-N-Amp tissue PCR kit (Sigma, 029K6262). Isolated DNA was then subjected to Polymerase Chain Reaction (PCR) using the reaction components outlined in Table 2.1. For $p27^{Kip1}$ PCR, the REDExtract-N-Amp PCR Reaction Mix (Sigma, R4775) was used and the components are outlined in Table 2.2.

The PCR reaction for Mcl-1 was programmed to be in 94°C for 6 minutes, 55°C for 1 minute and 72°C for 1 minute - repeated for 30 cycles. The PCR reaction for Cre was programmed to be in 94°C for 3 minutes, 56°C for 1 minute and 72°C for 1.5 minutes - repeated for 30 cycles. The PCR reaction for $p27^{Kip1}$ was programmed to be in 94°C for 6 minutes, 61°C for 1 minute and 72°C for 1 minute - repeated for 12 cycles, followed by 25 repetitions of 94°C for 3 minutes, 58°C for 1 minute and 72°C for 1 minute.

PCR products were run in a 2% agarose gel (UltraPure Agarose – Invitrogen, 15510-027) containing Ethidium bromide (15585-011, Invitrogen) to stain the DNA under ultraviolet light. The gel was run at 120 Volts for 30 minutes to detect the Cre band and for 90 minutes for the Mcl-1 band. $Mcl\text{-}1^{f/f}$ allele has two 34bp *lox*P sites flanking exon 1 (Opferman et al., 2005), as a result the wildtype $Mcl\text{-}1^{+/+}$ allele (360bp) is smaller than the $Mcl\text{-}1^{f/f}$ allele (400bp). Using the difference in the size of the bands under ultraviolet light, these two alleles can be distinguished. The wildtype $p27^{Kip1}$ ($p27^{Kip1\ +/+}$) band can be identified at 190bp compared to mutant $p27^{Kip1}$ ($p27^{Kip1\ -/-}$) band that can be identified at 280bp. Mice heterozygous for $p27^{Kip1}$ ($p27^{Kip1\ +/-}$) show both bands, one at 190bp and another at 280bp (Figure 2.2).

Reaction components	Volume /Sample (μL)	
	Mcl-1 PCR	Cre PCR
10x Reaction Buffer	5.0	5.0
Primers (2.5 μM):	Cre-3b* - 4.0 Cre-5b** - 4.0	Mcl-1 (6)# - 5.0 Mcl-1 (7)## - 5.0
1.25 mM dNTPs	8.0	8.0
50 mM $MgCl_2$	1.75	1.5
Taq Polymerase	0.5	0.5
Water	24.75	22.0
DNA sample	2.0	3.0
Cre-3b* = 5' TGA CCA GAG TCA TCC TTA GCG 3' Cre-5b** = 5' AAT GCT TCT GTC CGT TTG CC3' Mcl-1 (6)# = 5' GCA GTA CAG GTT CAA GCC GAT G3' Mcl-1 (7)## = 5' CTG AGA GTT GTA CCG GAC AA3'		

Table 2.1: Reaction components for Mcl-1 and Cre PCR

Reaction components	Volume /Sample (μL)
REDExtract-N-Amp PCR Reaction Mix	10.0
Primers (20 μM):	p27 wt-F* - 0.4 p27 wt-R** - 0.4 p27 mt-F# - 0.4 p27 mt-R## - 0.4
Water	8.4
DNA sample	4.0
p27 wt-F* = 5' GAT GGA GCG CAG ACA AGC 3' p27 wt-R ** = 5' CTC CTG CCA TTC GTA TCT GC3' p27 mt-F# = 5' CTT GGG TGG AGA GGC TAT TC3' p27 mt-R## = 5' AGG TGA GAT GAC AGG AGA TC3'	

Table 2.2: Reaction components for $p27^{Kip1}$ PCR

Figure 2.2: Identifying Mcl-1, Cre and $p27^{Kip1}$ genotype by PCR.

A - The floxed Mcl-1 ($Mcl\text{-}1^{f/f}$) allele can be distinguished from wildtype Mcl-1 ($Mcl\text{-}1^{+/+}$) allele by the difference in band size. $Mcl\text{-}1^{f/f}$ has two 34bp *loxP* sites and is seen as the larger band compared to $Mcl\text{-}1^{+/+}$. Mice that are heterozygous to Mcl-1 ($Mcl\text{-}1^{+/fl}$) show both bands.

B - Cre can be identified by the presence of a band at ~700bp.

C - Wildtype $p27^{Kip1}$ ($p27^{Kip1\ +/+}$) can be identified by a band at 190bp, compared to mutant $p27^{Kip1}$ ($p27^{Kip1\ -/-}$) that can be identified by a band at 280bp. Mice heterozygous for $p27^{Kip1}$ ($p27^{Kip1\ +/-}$) show both bands.

A

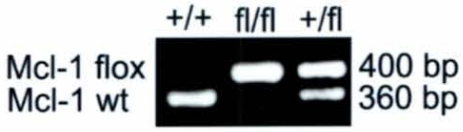
+/+ fl/fl +/fl
Mcl-1 flox
Mcl-1 wt
400 bp
360 bp

B

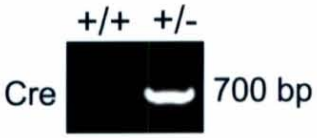
+/+ +/-
Cre
700 bp

C

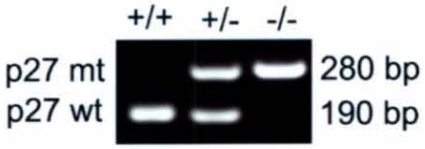
+/+ +/- -/-
p27 mt
p27 wt
280 bp
190 bp

2.3 Culturing clonally derived NPCs

NPCs were harvested from the neuroepithelia of the E 13 embryos. Pregnant dams were euthanized with a lethal intraperitoneal injection of Euthanyl (250 mg/mL sodium pentobarbital, Vètoquinol, IEUS001), followed by cervical dislocation. The uterus containing the embryos was dissected and submerged in cold 1x HBSS pH 7.4 (made from 10x HBSS – Hanks' Balanced Salt Solution; Gibco, 14065-056, and Gibco distilled water, 15230-162) with phenol red (Sigma, P0290). Individual embryos were removed from their embryonic sac and their brains extracted in cold 1x HBSS. The NPCs were harvested from the ganglionic eminences of these embryos by making a longitudinal incision through the overlying cortex. The excised ganglionic eminences were immediately transferred into stem cell media (SCM), prepared as described in Appendix I, and manually triturated to single cells. Cells were counted in a 1:1 mix with 0.4% Trypan Blue (Gibco, 15250-61) on a Hemacytometer (Fisher Scientific, 0267110). Neural precursor cells were then plated at clonal density (10 cells/μL) to grow neurospheres and incubated at 37°C with 5% carbon dioxide and humidity.

2.4 Plasmids Constructs

For studying Mcl-1 gain-of-function, a mutant Mcl-1 (mt Mcl-1) construct from (Zhong et al., 2005) was used where the lysine residues, involved in ubiquitin-mediated destruction of the protein, were converted to arginine. The pCIG2 expression vector (Megason and McMahon, 2002) (Appendix II) was used to direct the expression of mt Mcl-1 both *in vivo* and *in vitro*. The

mt Mcl-1 construct was cloned into the pCIG2 vector 5' to the internal ribosome entry sequence (IRES) and enhanced green fluorescent protein (eGFP) (Appendix III).

For studying $p27^{Kip1}$ gain-of-function, $p27^{Kip1}$ from pGFP-E p27 vector (Dyer and Cepko, 2001) was cloned into the pCIG2 vector 5' to the internal ribosome entry sequence (IRES) and enhanced green fluorescent protein (eGFP) (Appendix IV).

The expression of both pCIG2 mt Mcl-1 and pCIG2 $p27^{Kip1}$ were verified through transfection of E13 NPCs followed by protein analysis via Western Blot 24 hours post-transfection, as shown in Figure 2.3. The overexpressed mt Mcl-1 band (human) appears at 37 kDa while the endogenous Mcl-1 band (mouse) appears at 35 kDa as a doublet. Since the endogenous level of Mcl-1 is too low for performing protein interaction studies, all immunoprecipitation experiments were based on the overexpressed mt Mcl-1.

Figure 2.3: Verification of Mcl-1 and $p27^{Kip1}$ overexpression in E13 NPCs.

A - Western blot analysis of protein samples 24 hours post transfection with actin used as a loading control (42 kDa). The overexpressed Mcl-1 band (human) appeared at 37 kDa while the endogenous Mcl-1 band (mouse) appeared at 35 kDa.

Ctl = cells transfected with pCIG2 control plasmid, mt Mcl-1 = cells transfected with mt Mcl-1.

B - Western blot analysis of protein samples 24 hours post transfection with actin used as loading control (42 kDa). The $p27^{Kip1}$ band appeared at 27 kDa.

Ctl = cells transfected with pCIG2 control plasmid, $p27^{Kip1}$ = cells transfected with $p27^{Kip1}$.

A

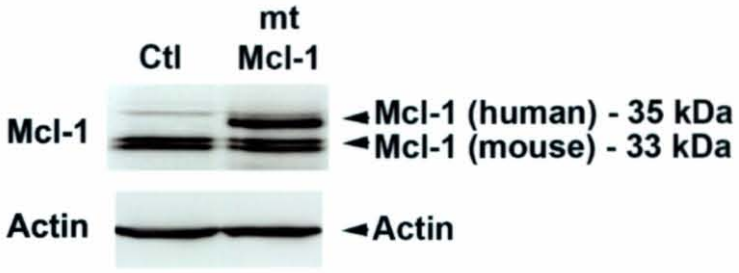
Ctl
mt Mcl-1
Mcl-1
Mcl-1 (human) - 35 kDa
Mcl-1 (mouse) - 33 kDa
Actin
Actin

B

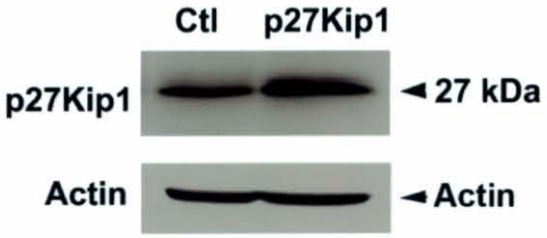
Ctl
p27Kip1
p27Kip1
27 kDa
Actin
Actin

2.5 *In vitro* Transfection of NPCs

3-4 days after plating, neurospheres were passaged to single cells and then transfected 24 hours later. Transfection was carried out using the Amaxa Mouse Neural Stem Cell Nucleofector Kit (Lonza, VPG-1004) and Amaxa Nucleofector Device (Lonza, AAD-1001), according to manufacturer's instruction. For every million ($1x10^6$) NPCs, 10 μg of plasmid DNA was used for transfection.

Transfected cells for protein assay were plated in stem cell media immediately following transfection. Cells for immunocytochemistry were plated immediately following transfection in stem cell media without heparin for adherent cultures.

2.6 *In vitro* Proliferation Assay

NPCs were transfected with pCIG2 control plasmid, mt Mcl-1 plasmid or $p27^{Kip1}$ plasmid and plated in proliferating conditions at clonal density, on Poly-ornithine (Sigma, P4957) coated dishes. To determine the effects of Mcl-1 gain-of-function on proliferation, transfected NPC cultures received a 5-Bromo-2-deoxyuridine (1mM BrdU – Sigma, B5002) pulse 2 hours immediately before fixation. Cultures were fixed with 1:1 methanol (Sigma, 179337-4L) and acetone (Fisher Scientific, A949-4) at 24 hours, 48 hours or 72 hours post transfection.

Proliferation was assessed to compare the effects of Mcl-1 or $p27^{Kip1}$ gain-of-function on NPCs. This was performed using immunocytochemistry for proliferating cell nuclear antigen (PCNA) at 24 hours, 48 hours or 72 hours post transfection.

2.7 Protein extraction from cultures

Protein samples were extracted from NPCs. Cells were lysed in complete immunoprecipitation (IP) buffer containing 25 mM Tris-Base pH 7.4, 148 mM NaCl, 1 mM $CaCl_2$, 1% Triton X-100, 0.2 mg/mL phenylmethylsulfonyl fluoride (PMSF), 10X protease inhibitors (aprotinin and leupeptin) and 10 mM dithiothreitol (DTT). Samples were run in duplicates using Bio-Rad Protein Assay Reagent (BioRad, 500-0006) to determine the protein concentration of each sample by producing a standard curve using the Bradford Assay (Table 2.3).

Tube	dd H_2O (µL)	BSA Standard (µL)	Bio-Rad reagent (µL)	Approx. Absorbance
1	800	0	200	0.000
2	795	5	200	0.150
3	790	10	200	0.300
4	785	15	200	0.450
Sample (5 µL)	795	0	200	

Table 2.3: Bradford Assay Standard Curve

The slope of the standard curve was used to determine protein concentration of each sample using the following equation:

$$\text{Sample Concentration} \left(\frac{\mu g}{\mu L}\right) = \frac{\text{(Mean sample absorbance)}}{\text{(Slope) (Volume of sample)}} * \text{Dilution Factor}$$

2.7 Immunoprecipitation with Protein-G Sepharose Beads

Individual protein samples containing 600 μg of protein in 250 μL of complete IP buffer, 5 μg of specific antibodies (Cyclin dependent kinase 1 (Cdk1) - Santa Cruz, SC53219; Cyclin B – Santa Cruz, SC752; Mcl-1 – Santa Cruz, SC819) were used for pulling down protein complexes. Proteins with antibodies were placed on a rotator at 4°C for 3 hours, then 40 μL of Protein G Sepharose Beads (Sigma, P3296-1mL) were added and set back to incubate overnight. The following day, beads were washed in cold complete IP buffer to remove any non-specific binding and then centrifuged at 1000 rpm for 2 minutes in 1°C, allowing the specific protein complexes bound to the antibodies and beads to sediment. To this pellet, 40 μL of 6X protein loading buffer (250 mM Tris-HCl, 0.5M DTT, 10% Sodium dodecyl sulphate (SDS), 0.5% bromophenol blue and 50% glycerol) was added. Samples were boiled at 100°C for 2 minutes to dissociate the protein complexes, cooled to room temperature and then centrifuged at 10,000 rpm to sediment the sepharose beads. The supernatant containing the protein samples was then loaded into 15% poly-acrylamide gel and was run according to the procedure for western blot.

2.8 Western Blot Analysis

Protein samples containing 60 μg of protein were mixed with 5μL of 6X protein loading buffer, boiled at 100°C for 2 minutes and then loaded on a 15% poly-acrylamide gel.

15% Separating gel	
dd water	4.5ml
0.5M Tris, 1.5M glycine	4.0ml
10% SDS	0.8ml
50% glycerol	2.0ml
40% acrylamide; 0.25% bisacrylamide	7.0 ml
Ammonium persulphate	30mg in 1 ml of water
TEMED	0.02ml
4% Stacking gel	
dd water	4.05ml
0.5 M Tris-HCl pH 6.8	1.4ml
10% SDS	0.4ml
50% glycerol	1.0ml
40% acrylamide, 0.25% bisacrylamide	1.25ml
Ammonium persulphate	25mg in 1ml of water
10% TEMED	0.01 ml

Table 2.4: Recipes for Poly-acrylamide separating and stacking gels

A Mini-PROTEAN apparatus (BioRad, 165-8001) filled with Running Buffer (0.1 M Tris-Base, 0.3 M glycine, 0.01 M SDS) was used to run the gel. The protein samples were loaded into the stacking gel and run at 80 volts until the dye cleared the stacking gel. Once the samples reached the separating gel, the gel was run at 110 volts for 3 hours. To determine the size of various protein bands, 10 µL of Bio-Rad Kaleidoscope pre-stained protein marker (Bio-Rad, 161-0324) was also loaded in one of the lanes in each gel.

Proteins from the separating gel were transferred to a nitrocellulose membrane (Amersham BioSciences, RPN30320) with the BioRad Mini Trans-Blot Electrophoretic Transfer Cell (BioRad, 170-3930) in Western Transfer Buffer (0.02 M Tris-Base, 0.15 M glycine and 4.9 M methanol). Following transfer, the membrane was washed in 1x Tween-20 phosphate buffered saline, TPBS (126 mM NaH_2PO_4, 620 mM NaCl, 4 mM Tween-20, ddH_2O) for 15 minutes on the shaker, then blocked in 5% blotto (5% skim milk in TPBS) for an hour at room temperature, followed by a wash in 0.5% blotto. Blots were incubated overnight with appropriate primary

antibody (Appendix V) in 0.5% blotto at 4°C in a sealed plastic container on a shaker at low speed.

The following day, membranes were washed in 0.5% blotto, followed by incubation with appropriate secondary antibody (1:2000 goat anti-rabbit IgG horseradish peroxidase (HRP) conjugate, BioRad, 1706515; 1:2000 goat anti-mouse IgG HRP conjugate, BioRad, 1706516) diluted in 0.5% blotto for 1 hour in room temperature. Then membranes were washed in 1x TPBS and the secondary antibodies were detected using a chemiluminescence reaction kit (Perkin Elmer Labs Inc. – Western Lightning, 02118-2512) according to the manufacturer's instructions. Images of the membranes were taken 1 minute after applying the chemiluminescence reagent, using GE ImageQuant LAS 4000 (GE Healthcare, 28-9558-10). To detect the levels of β-actin, the loading control, membranes were stripped using Western Blot Stripping Buffer (Sigma, 21059) at 37°C for 30 minutes and the procedure was repeated following a wash in 5% blotto.

2.9 *In utero* electroporation

In utero electroporation was performed on pregnant CD-1 female mice at E13 (embryonic day 13), to examine the effects of Mcl-1 gain-of-function on neural precursor cells *in vivo*. Pregnant females were anaesthetized with isofluorane inhalation and were closely monitored during the entire procedure. A hypotear ophthalmic ointment was applied on the eyes of the mouse during the surgical procedure to prevent eyes from drying out. The entire procedure was performed within 45 minutes. During the surgery, the mouse was kept on a sterile padding on a heating pad set at 30°C to maintain body temperature.

Once anaesthetized, the fur was removed from the abdomen of the pregnant mouse using Nair (Church & Dwight Canada Corp., Mississauga, ON). The abdomen was then cleared with 70% ethanol and an incision was made down the midline of the abdomen and through the intraperitoneal wall, which was then lined with sterile gauze. Uterine horns were pulled through the incision and placed on sterile gauze and moistened with pre-warmed sterile 0.9% saline. Individual embryos received an injection of the plasmid (1μg/μL), either pCIG2 control, $p27^{kip1}$ or mt Mcl-1 plasmids, using a FemtoJet Injector (100hPa, 1.2 sec, PC=16) into the laterai ventricles. The plasmid solution also contained a non-toxic dye to visually monitor injections into the lateral ventricles. Following the injection, electroporation paddles (5mm, Protech International, CUY650P5) were placed on opposite poles of the embryo's head and using an ECM 830 Generator (Harvard Apparatus) a series of 7 pulses at 45 volts, 50 msec duration with a 500 msec interval, were delivered as described previously (Langevin *et al.* 2007). Following electroporation, the uterine horn was re-inserted back into the abdomen of the pregnant mouse, the musculature and overlying skin sutured and the mouse was allowed to recover. At completion of the surgery, a topical gentamicin (Topagen) was sprayed on the abdomen of the pregnant mouse to minimize infection of the wound.

Post surgery mice were given sterilized drinking water with sulfamethazine antibiotic (0.05% sodium sulfamethazine solution) for the first 3 days post-operation to prevent infection. The health and weight of the mice were monitored on a daily basis until euthanasia. 24 hours post-electroporation, pregnant mice received a single intraperitoneal BrdU injection (100μg/g body weight) to label proliferating cells. Brains of the electroporated embryos were collected at 48 hours and 5 days following the *in utero* electroporation, or two weeks postnatally.

2.10 Tissue collection, fixation, cryoprotection and sectioning

At 48 hours and 5 days following the *in utero* electroporation, pregnant mice were euthanized with a lethal intraperitoneal injection of Euthanyl (250 mg/mL sodium pentobarbital, Vètoquinol, IEUS001), followed by cervical dislocation. The uterus was removed by making an incision through the abdominal wall and placed in 1x PBS. The embryos were removed from the embryonic sacs and their brains dissected. Brains were checked under the microscope for GFP fluorescence, and only those with GFP expression were collected. Pups collected 2 weeks postnatally were also sacrificed with a lethal intraperitoneal injection of Euthanyl. Following euthanasia, pups were perfused with ice-cold 1x PBS followed by 4% Para-formaldehyde (PFA – Fisher Scientific, 04042-500; 1x PBS, dd H_2O, pH 7.4).

Brains were post fixed overnight in 4% PFA. After fixation, the tissue was cryoprotected by equilibrating in increasing concentrations of sucrose solutions (12%, 16% and 22% w/v sucrose in 1x PBS). Following cryoprotection, brains were frozen in Tissue-Tek (Sakura Finetek, 0004348-01) on isopentane, cooled on dry ice. Brains were sectioned (14 µm in thickness) on the same day as freezing, on a cryostat (Microm HM 520 Cryostat). Tissue sections were collected on Superfrost Plus (Fisherbrand, 12-550-15) slides and then stored at -80°C until further processing.

2.11 Immunohistochemistry and Immunocytochemistry

For immunohistochemistry, slides were warmed to 37°C and a hydrophobic moat (Dako pen) was drawn around the brain sections. For nuclear stains (PCNA, Tbr1, BrdU and Cux1), slides were

post-fixed in acetone (Fisher Scientific, A949-4) for one minute followed by washes in 1x PBS. Slides were next incubated overnight with primary antibodies (Appendix V) diluted in 1x PBS at room temperature. For BrdU and PCNA (proliferating cell nuclear antigen) immunohistochemistry, slides were pre-treated in 2N HCl for 30 minutes at 37°C followed by 0.1 M $Na_2B_4O_7$ (pH 8.0) wash for 10 minutes to denature the DNA. Slides were then washed in 1x PBS before incubating overnight with primary antibody in the humidity chamber at room temperature.

For PCNA immunocytochemistry, cultures were fixed using cold (-20°C) 1:1 methanol:acetone (Fisher Scientific, A949-4) for 5 minutes. This was followed by washes in cold (4°C) 1x phosphate buffered saline (PBS – 137 mM NaCl, 27 mM KCl, 100 mM Na_2HPO_4, 18 mM KH_2PO_4, dd H_2O, adjusted to pH 7.4). Then the cells were first treated with 2N Hydrochloric acid (Fisher Scientific, SA56500) at room temperature for 15 minutes followed by washes in cold 1x PBS. Following this, primary antibodies for PCNA (1:300 – Vector Labs, VP-P980) in 1x PBS was added to the cells and incubated overnight at 4°C.

For BrdU immunocytochemistry, cultures were fixed using cold (4°C) 4% PFA for 10 minutes, followed by washes in cold (4°C) 1x PBS. Then the cells were treated with DNase (1 unit/50 µL - Promega, M6101) in DNase Buffer (40 mM Tris-Hcl, 10 mM NaCl, 6 mM $MgCl_2$ and 10 mM $CaCl_2$) at 37°C for 30 minutes, to denature the DNA. Following this, cells were washed in 1x PBS and then incubated with primary antibodies for BrdU (1:100 – BD Biosciences, 347580) in 1x PBS overnight at 4°C.

The following day, the slides or culture dishes were washed in 1x PBS and incubated with the appropriate secondary antibody diluted in 1x PBS (1:200 donkey anti-mouse IgG (H+L) Alexa Fluor 594 – Invitrogen, A21203; 1:200 donkey anti-rabbit IgG (H+L) Alexa Fluor 594 –

Invitrogen, A21207) for one hour, covered with aluminium foil. Following this, the cells were stained with the nuclear dye Hoechst diluted in 1x PBS (1:250 BisBenzimide H33258 – Sigma, B1155) for two minutes and then washed again in 1x PBS. Slides were then coverslipped with 1:3 glycerol:1x PBS and the edges were sealed with nailpolish.

2.12 Microscopy and Statistics

Cultures were examined on a Zeiss AxioObserver A.1 microscope to confirm transfection and subsequent expression of plasmids. Immunostained cells and tissues were examined on a Zeiss AxioImager Z.1 microscope under LED fluorescence produced using Colibri. Each slide contained three brain sections, each about 140 μm apart. Photomicrographs were taken of each embryonic brain section at the same magnification. The sample size indicates the number of different embryos used for each treatment group. Average number of GFP^+ cells detected per experiment for each treatment group is listed in Appendix VI.

All images were taken with Zeiss AxioCam MRm camera using Zeiss AxioVision 4.8 software. Images were processed and the figures were compiled using Adobe Photoshop CS2 where manipulations were made only to contrast and brightness. The freeware Image J (National Institute for Health) was used for quantification of positive cells following immunostaining and the counts were maintained in Microsoft Excel spreadsheets. All statistics were performed using GraphPad Prism 5 software, including unpaired T-test and One-way Analysis of Variance (ANOVA). Tukey's post hoc analysis was used to determine differences between treatment groups.

Chapter 3

Results

3.1 How does Mcl-1 affect embryonic NPCs in vivo?

During neurogenesis within the embryonic brain, NPCs divide at the ventricular zone (VZ) and subventricular zone (SVZ). As NPCs exit the cell cycle and progress towards a neuronal lineage, they migrate radially out into the cortical plate (CP) (Malatesta et al., 2008). Therefore, the proliferating zones in the developing cortex are the VZ and SVZ, while the post-mitotic differentiated cells make up the CP.

To investigate the effects of Mcl-1 gain-of-function on NPCs, I electroporated GFP (control) or mt Mcl-1 plasmids into E13 mouse embryos *in utero*. I collected the brains 48 hours post electroporation and assessed the location of the GFP^+ transfected cells.

In control brains, the distribution of GFP^+ cells was mostly in the proliferative zones, VZ (26±2%) and SVZ (52±2%), with less than a fourth of the GFP^+ cells in the post-mitotic CP (21±3%). In contrast, there was a shift in the location of the GFP^+ cells towards the CP in the mt Mcl-1 treated brains. Less than half of the GFP^+ cells in mt Mcl-1 treated brains were in the proliferative zones, VZ (16±2%) and SVZ (26±2%), and most of GFP^+ cells were in the CP (58±3%) (Figure 3.1). This distinct shift in the location of GFP^+ cells in the mt Mcl-1 treated brains suggested that Mcl-1 gain-of-function induces NPCs to exit the cell cycle and migrate to the CP.

Figure 3.1: Mcl-1 gain-of-function promotes migration of NPCs into the cortical plate.

A – Representative photomicrographs of embryonic brain sections 48 hours post-electroporation of control (Ctl) or mt Mcl-1 plasmids, showing the location of GFP^+ cells in the VZ (ventricular zone), SVZ (subventricular zone) and CP (cortical plate).

B – Quantification of the percent GFP^+ cells located in VZ, SVZ and CP within Ctl and mt Mcl-1 treated brains. GFP^+ cells were counted in 3 representative sections per embryo (n=5/treatment). Mean cell counts were analyzed by t-test with statistical significance assessed at $*p<0.05$. Graphs represent means ±SEM.

A

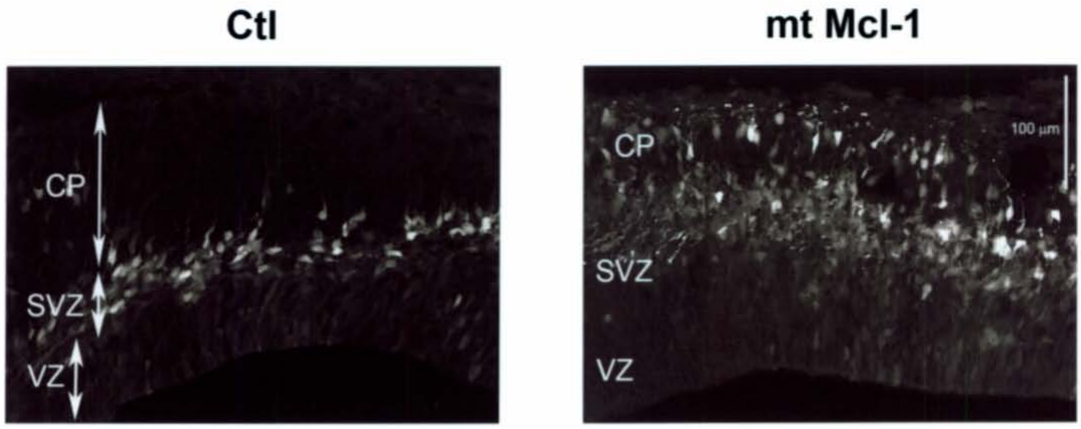
Ctl
mt Mcl-1
CP
SVZ
VZ
100 μm
CP
SVZ
VZ

B

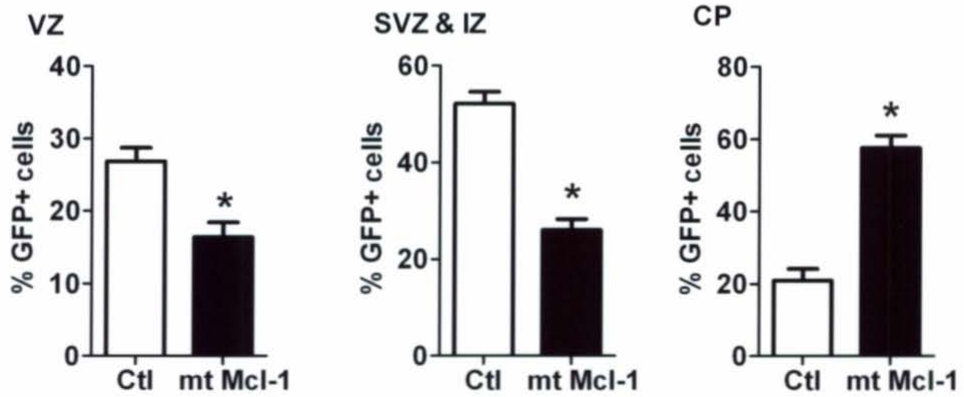
VZ
% GFP+ cells
40
30
20
10
0
*
Ctl
mt Mcl-1
SVZ & IZ
% GFP+ cells
60
40
20
0
*
Ctl
mt Mcl-1
CP
% GFP+ cells
80
60
40
20
0
*
Ctl
mt Mcl-1

3.2 Mcl-1 regulates NPC proliferation within the embryonic brain

To characterize the effect of Mcl-1 on embryonic NPC proliferation, I electroporated GFP (control) or mt Mcl-1 plasmids into E13 mouse embryos *in utero* and assessed proliferation with PCNA immunohistochemistry 48 hours post electroporation. PCNA is a component of DNA polymerase-delta and is required for DNA replication. As a result, there is a distinct increase in PCNA expression during the S-phase (Bacchi and Gown, 1993) and so it is used widely as a marker for cell proliferation. 48 hours post electroporation, in control brains 22±3% of transfected cells were also $PCNA^+$. In contrast, only 8±1% of transfected cells were also $PCNA^+$ in the mt Mcl-1 treated brains (Figure 3.2). This greater than two-fold reduction in proliferating NPCs suggests that Mcl-1 gain-of-function promotes cell cycle exit of NPCs.

Figure 3.2: Mcl-1 regulates NPC proliferation in the embryonic brain.

A – Representative photomicrographs of embryonic brain sections 48 hours post electroporation showing GFP^+ cells and $PCNA^+$ cells in control and mt Mcl-1 electroporated brains. Arrows point to double labeled cells.

B – Quantification of the percent double labeled GFP^+ and $PCNA^+$ cells in control (Ctl) and mt Mcl-1 electroporated brains. GFP^+ cells were counted in 3 representative sections per embryo (n=5/treatment). Mean cell counts were analyzed by t-test with statistical significance assessed at $*p<0.05$. Graphs represent means ±SEM.

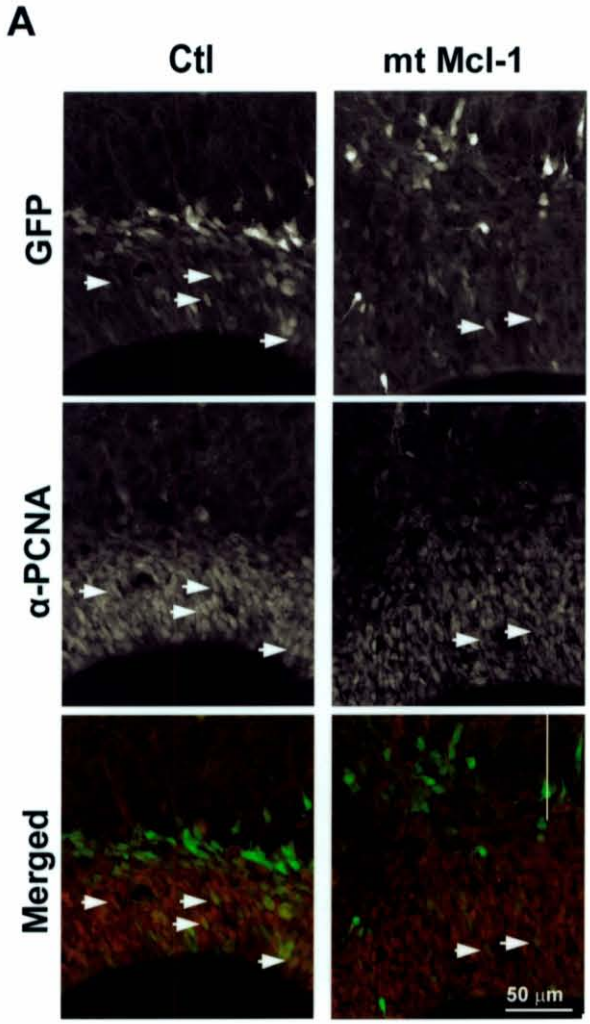
A
Ctl
mt Mcl-1
GFP
α-PCNA
Merged
50 μm
B
% PCNA+ & GFP+ cells
30
20
10
0
*
Ctl
mt Mcl1

3.3 Mcl-1 promotes NPC differentiation within the embryonic brain

Since Mcl-1 gain-of-function reduces NPC proliferation, I assessed if Mcl-1 regulates NPC differentiation. The stages of neurogenic progression of a NPC can be distinguished by sequential expression of specific transcription factors (Figure 1.2). The expression of the Tbr1 transcription factors confirms the neurogenic transition of NPCs and can be used to label newborn neurons (Hevner et al., 2006). I electroporated GFP (control) or mt Mcl-1 plasmids into E13 mouse embryos *in utero* and assessed differentiation with Tbr1 immunohistochemistry 48 hours post electroporation. In control brains 18±3% of transfected cells were also $Tbr1^+$. In contrast, 29±3% of transfected cells were $Tbr1^+$ in the mt Mcl-1 treated brains (Figure 3.3). The 50% increase in differentiated neurons within mt Mcl-1 electroporated brains suggests that Mcl-1 gain-of-function promotes neurogenesis.

Figure 3.3: Mcl-1 promotes NPC differentiation in the embryonic brain.

A – Representative photomicrographs of embryonic brain sections 48 hours post electroporation showing GFP^+ cells and $Tbr1^+$ cells in control and mt Mcl-1 electroporated brains. Arrows point to double labeled cells.

B – Quantification of the percent double labeled GFP^+ and $Tbr1^+$ cells in control (Ctl) and mt Mcl-1 electroporated brains. GFP^+ cells were counted in 3 representative sections per embryo (n=5/treatment). Mean cell counts were analyzed by t-test with statistical significance assessed at $*p<0.05$. Graphs represent means ±SEM.

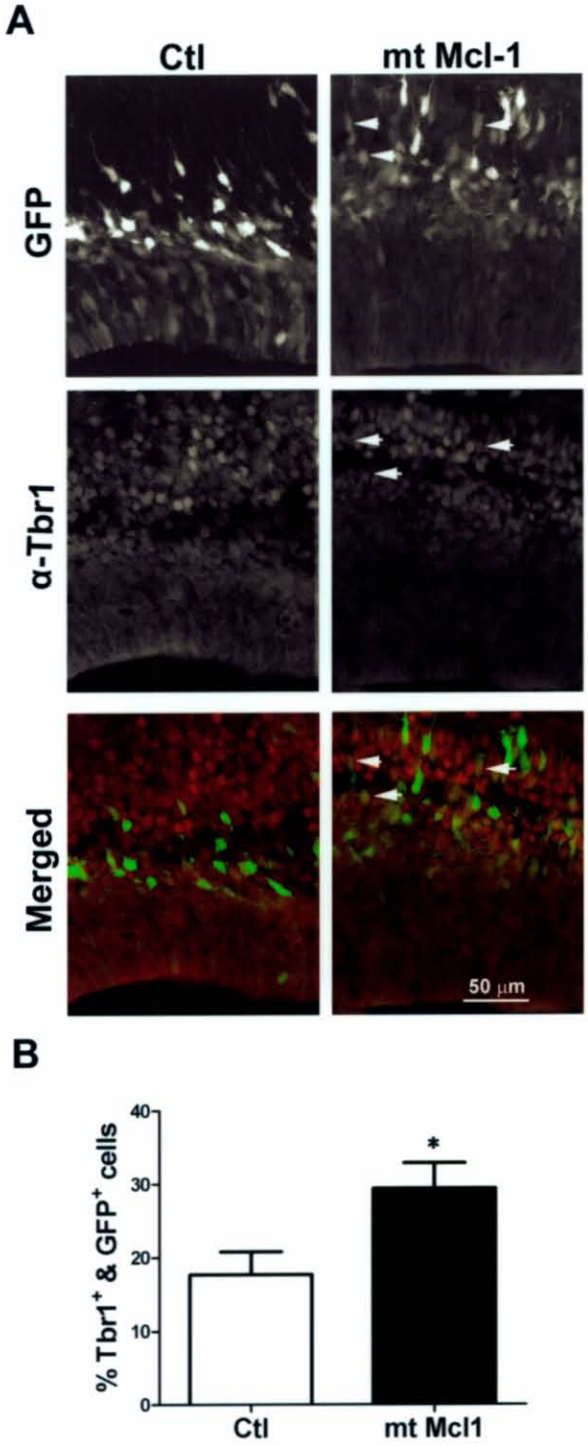
A
Ctl
mt Mcl-1
GFP
α-Tbr1
Merged
50 μm
B
% Tbr1+ & GFP+ cells
40
30
20
10
0
*
Ctl
mt Mcl1

3.4 Mcl-1 gain-of-function generates a greater cohort of newborn cells

Since Mcl-1 gain-of-function promotes neuronal differentiation of NPCs, I examined if transfected NPCs prematurely exit their cell cycle and become post-mitotic. This was performed with a BrdU birthdating experiment. Electroporation was performed on E13 mouse embryos and pregnant dams were administered a single BrdU pulse 24 hours post electroporation. BrdU labels dividing cells as they undergo DNA replication in S-phase. Proliferating cells dilute the BrdU label with each successive division, whereas cells in their last mitotic division at the time of injection retain the BrdU label and are considered "born" at that time. I assessed the embryos 5 days post electroporation, when the only cells to retain the BrdU signal are the cells that have exited the cell cycle at the time of injection. Immunohistochemistry for BrdU revealed that in control brains 6±1% of transfected cells were also $BrdU^+$. In contrast, 14±2% of transfected cells were $BrdU^+$ in the mt Mcl-1 treated brains (Figure 3.4). Therefore, Mcl-1 gain-of-function generated a 2-fold greater cohort of newborn cells. These results demonstrated that Mcl-1 promotes NPCs to prematurely exit the cell cycle.

Figure 3.4: Mcl-1 gain-of-function generates a greater cohort of newborn cells.

A – Representative photomicrographs of embryonic brain sections 5 days post electroporation showing GFP^+ cells and $BrdU^+$ cells in control and mt Mcl-1 electroporated brains. Pregnant dams received a single BrdU pulse 24 hours post electroporation. Arrows point to double labeled cells.

B – Quantification of the percent double labeled GFP^+ and $BrdU^+$ cells in control (Ctl) and mt Mcl-1 electroporated brains. GFP^+ cells were counted in 3 representative sections per embryo (n=5/treatment). Mean cell counts were analyzed by t-test with statistical significance assessed at $*p<0.01$. Graphs represent means ±SEM.

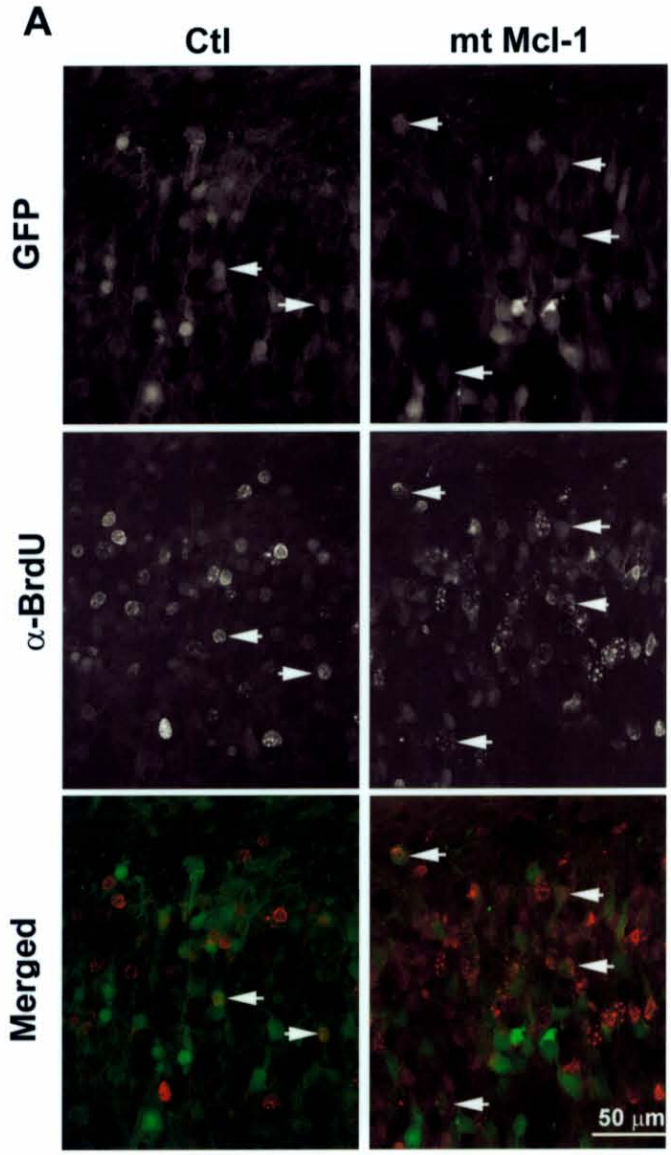
A
Ctl
mt Mcl-1
GFP
α-BrdU
Merged
50 μm

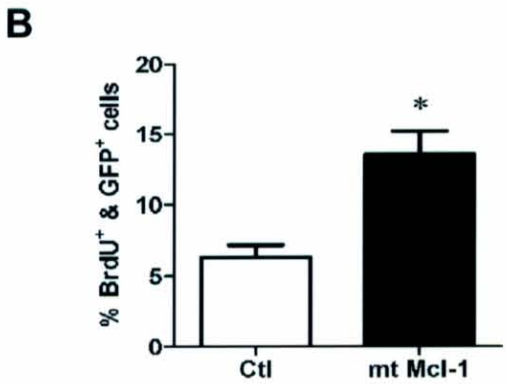
B
% BrdU+ & GFP+ cells
20
15
10
5
0
*
Ctl
mt Mcl-1

3.5 Mcl-1 gain-of-function alters the laminar destination of NPCs in the developing cortex

Since Mcl-1 gain-of-function promotes premature cell cycle exit of NPCs, I examined the final laminar location of transfected cells in the developed cortex. Electroporation was performed on E13 embryos and the pups were collected 2 weeks post-natally. Corticogenesis in mice is from E11-E19 (Dehay and Kennedy, 2007) and there is a second wave of apoptosis among differentiated neurons (de la Rosa and de Pablo, 2000, Blomgren et al., 2007) following corticogenesis. Therefore, the 2 week post-natal time point allowed assessment of the location of transfected cells that have survived.

Laminar location of the GFP^+ cells were identified using a layer specific marker, Cux1 (Cut like transcription factor), that labels cortical layers II-IV (Leone et al., 2008). Cells born on E15 or later make up the neurons in the $Cux1^+$ upper cortical layers II-IV. Cells born at an earlier time make up the deeper cortical layers V-VI (Caviness et al., 2009), as the cortex develops "inside-out". Immunohistochemistry for Cux1 revealed that in control brains almost all the GFP^+ cells (98±1%) were in the upper cortical layers II-IV. In contrast, only 81±2% of transfected cells were in the upper cortical layers II-IV in the mt Mcl-1 treated brains. The remaining 18±2% of transfected cells were in the deeper layers V-VI, confirming their earlier birthdate (Figure 3.5). This is consistent with my previous data that Mcl-1 gain-of-function promotes premature cell cycle exit of NPCs in the embryonic brain.

Figure 3.5: Mcl-1 gain-of-function alters the laminar destination of NPCs.

A – Representative photomicrographs of brain sections from 2 week-old postnatal pups showing GFP^+ cells and $Cux1^+$ cells in cortical layers II-IV in control (Ctl) and mt Mcl-1 treated brains. Electroporation was performed on E13 embryos.

B – Quantification of the percent of GFP^+ cells in layers II-IV and layers V-VI. GFP^+ cells were counted in 3 representative sections per pup (n=5/treatment). Mean cell counts were analyzed by t-test with statistical significance assessed at $*p<0.01$. Graphs represent means ±SEM.

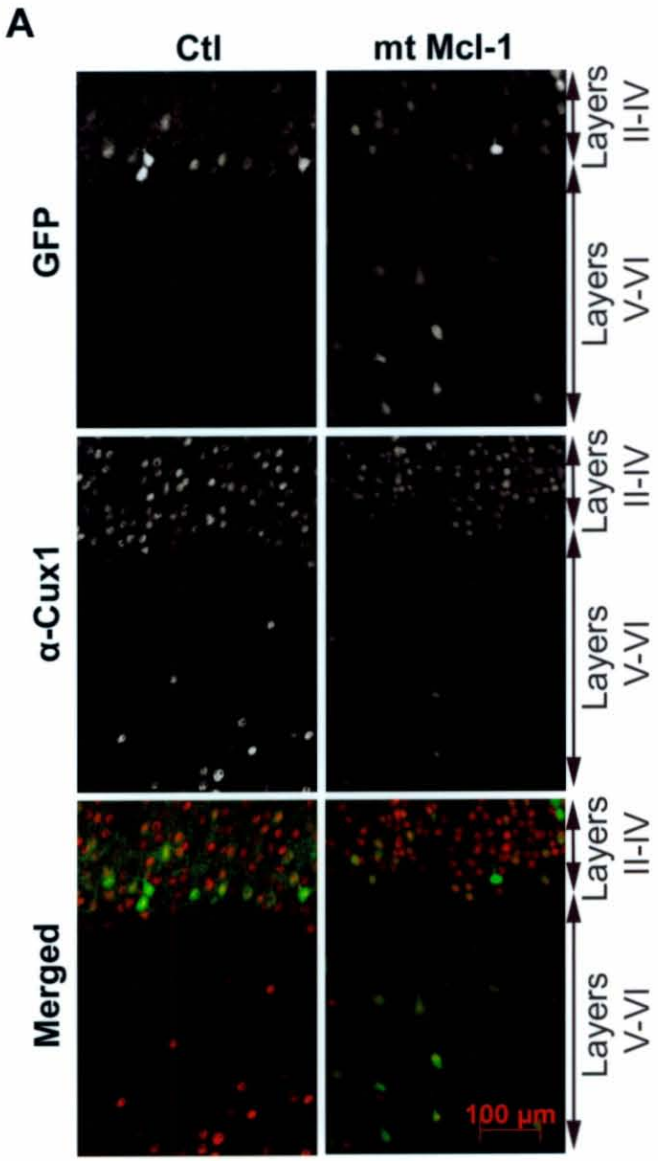
A
Ctl
mt Mcl-1
GFP
α-Cux1
Merged
Layers II-IV
Layers V-VI
100 µm
B
% GFP+ cells
100
80
60
40
20
0
*
*
Ctl
mt Mcl-1
Layer II - IV
Layer V - VI

3.6 Mcl-1 gain-of-function regulates NPC proliferation *in vitro*

The *in vivo* data revealed that Mcl-1 promotes premature cell cycle exit of NPCs that form the deeper cortical layers, confirming an earlier birthdate. So, I investigated if the cell cycle exit is cell autonomous for NPCs when replicated *in vitro*. I cultured E13 NPCs and transfected them with either control or mt Mcl-1 plasmid. To maintain transfected NPCs under proliferating conditions, I cultured them in a high concentration of FGF-2, a potent growth factor that promotes NPC proliferation (Tropepe et al., 1999, Sosunov and Chelyshev Iu, 2002).

The cultures received a BrdU pulse 2 hours before fixation at 24 and 48 hours following transfection of NPCs. BrdU labels the cells in S-phase. Immunocytochemistry for BrdU was carried out and the $BrdU^+$ transfected cells were quantified. In the control cultures 31±6% of GFP^+ cells were also $BrdU^+$ at 24 hours post transfection. Comparatively, only 12±1% of GFP^+ cells were $BrdU^+$ in the mt Mcl-1 treated cultures 24 hours post transfection. 48 hours post transfection, 31±1% of transfected cells were also $BrdU^+$ in control cultures, whereas only 14±2% of transfected cells were $BrdU^+$ in mt Mcl-1 treated brains (Figure 3.6). The 2-fold reduction in proliferation upon Mcl-1 overexpression at both 24 and 48 hours post transfection supported our *in vivo* findings that Mcl-1 promotes cell cycle exit of NPCs. Furthermore, this *in vitro* analysis also suggests that Mcl-1 promotes cell cycle exit independent of external cues. Therefore, Mcl-1 promotes cell cycle exit of NPCs through a cell autonomous manner.

Figure 3.6: Mcl-1 regulates NPC proliferation through a cell autonomous mechanism.

Quantification of the percent of GFP^+ cells that are also $BrdU^+$ in control (Ctl) and mt Mcl-1 transfected NPC cultures. Cultures received a 2 hour BrdU pulse before fixation at 24 hours or 48 hours post transfection. Proliferation was assessed with BrdU immunocytochemistry (n=5/treatment). Mean cell counts were analyzed by t-test with statistical significance assessed at *$p<0.01$. Graphs represent means ±SEM.

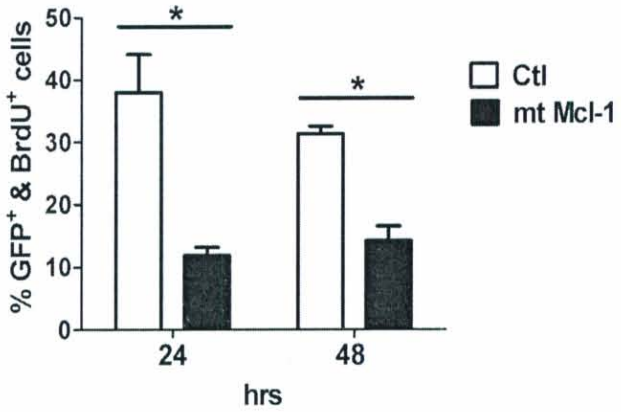
% GFP+ & BrdU+ cells
50
40
30
20
10
0
*
*
24
48
hrs
Ctl
mt Mcl-1

3.7 Mcl-1 directly interacts with cell cycle regulators in NPCs

Evidence of Mcl-1 interacting with cell cycle regulators comes either from forced expression of Mcl-1 in cell lines or from studies inducing cell cycle arrest. Mcl-1 slows cell cycle progression by binding to PCNA (Fujise et al., 2000) and Cdk1 (Jamil et al., 2005) in cell lines. In addition, during mitotic arrest, the Cdk1-Cyclin B1 complex binds to Mcl-1 promoting its phosphorylation (Harley et al., 2010). To determine whether Mcl-1 binds to either PCNA or Cdk1-Cyclin B1 in NPCs, I performed immunoprecipitation studies (Figure 3.7).

I transfected E13 NPCs with either control or mt Mcl-1 plasmid and collected the cells 24 hours post transfection. Immunoprecipitation was carried out with antibodies for Mcl-1, Cdk1 and Cyclin B1. A pre-IP sample was collected for western analysis to demonstrate the overall level of each protein in the lysates. Although Mcl-1 showed direct binding to PCNA in NPCs, there was no difference in this interaction with Mcl-1 overexpression (Figure 3.7A). In contrast, Mcl-1 sequestered more Cdk1-Cyclin B1 complex when overexpressed. This was demonstrated by immunoprecipitation for Mcl-1 and subsequent western analysis for Cdk1 or Cyclin B1 on the same blot (Figure 3.7B). This interaction was further confirmed by doing the reverse: immunoprecipitation for either Cdk1 or Cyclin B1 followed by western analysis for Mcl-1 (Figure 3.7C,D). Since Mcl-1 gain-of-function sequesters more Cdk1 and Cyclin B1 in NPCs, this may suggest a mechanism by which Mcl-1 regulates cell cycle progression of NPCs.

3.8 Changes in Mcl-1 expression show concomitant changes in $p27^{Kip1}$ expression

Previous *in vitro* studies in cell lines suggested that forced expression of Bcl-2 and Bcl_{XL} slows cell cycle progression by lengthening G1 phase. This effect on cell cycle was attributed to the increased level of $p27^{Kip1}$ expression, a G1 Cdk inhibitor (Vairo et al., 2000, Greider et al., 2002). $P27^{Kip1}$ is a key regulator of NPC cell cycle exit. Overexpression of $p27^{Kip1}$ promotes premature NPC cell cycle exit and alters their laminar destination (Goto et al., 2004). In contrast, knockout of $p27^{Kip1}$ causes increased NPC proliferation resulting in bigger brains (Tarui et al., 2005). So I questioned whether Mcl-1 affected NPC cell cycle by modulating the expression of $p27^{Kip1}$.

To assess this, I carried out both gain-of-function and loss-of-function approaches (Figure 3.8). Wildtype NPCs were transfected with either control or mt Mcl-1 plasmid and collected 24 hours post transfection. Western analysis was carried out on protein lysates from transfected NPCs and elevated levels of $p27^{Kip1}$ protein was observed upon Mcl-1 overexpression. For the loss-of-function model, NPCs were cultured from Mcl-1 conditional KO embryos and littermate controls. Western analysis of these NPCs shows a concomitant decrease in $p27^{Kip1}$ expression in the absence of Mcl-1. Taken together, this demonstrates that changes in Mcl-1 protein may affect the expression or stability of $p27^{Kip1}$ protein.

Figure 3.8: Changes in Mcl-1 expression show concomitant changes in $p27^{Kip1}$ protein in NPCs.

Western Blot analysis of $p27^{Kip1}$ and Mcl-1 protein expression in NPCs from E13 Mcl-1 conditional KO embryos (-/-), littermate controls (+/+), and in NPCs transfected with either control (Ctl) or mt Mcl-1 plasmids and collected 24 hours post transfection. Actin is used as the loading control. Blots are representative of 3 separate experiments.

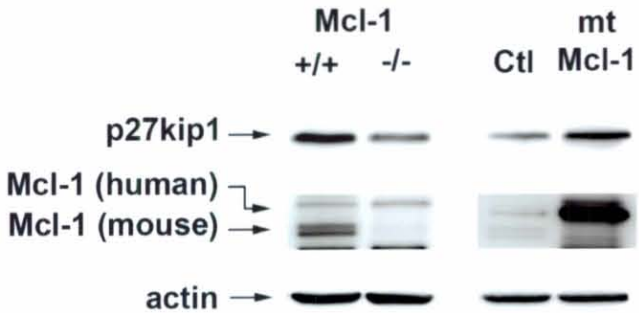
Mcl-1
+/+
-/-
mt
Ctl
Mcl-1
p27kip1
Mcl-1 (human)
Mcl-1 (mouse)
actin

3.9 $p27^{Kip1}$ affects NPC proliferation and differentiation similar to Mcl-1 *in vivo*

Since $p27^{Kip1}$ is a key promoter of NPC cell cycle exit and shows concomitant changes in protein with Mcl-1 expression, I asked if $p27^{Kip1}$ acts downstream of Mcl-1 to promote cell cycle exit of NPCs. To assess this, I first investigated the effects of $p27^{Kip1}$ gain-of-function on E13 NPCs *in vivo*. I electroporated GFP (control) or $p27^{Kip1}$ plasmids into E13 mouse embryos *in utero*. I collected the brains 48 hours post electroporation and assessed the location of the GFP^+ transfected cells.

In control brains, the distribution of GFP^+ cells was mostly in the proliferative zones, VZ (33±2%) and SVZ (44±2%), with less than a fourth of the GFP^+ cells in the post-mitotic CP (23±2%) (Figure 3.9A). In contrast, there was a shift in the location of the GFP^+ cells towards the CP in the $p27^{Kip1}$ transfected brains. Less than half of the GFP^+ cells in $p27^{Kip1}$ treated brains were in the proliferative zones, VZ (18±1%) and SVZ (30±1%), and most of GFP^+ cells were in the CP (52±2%) (Figure 3.9A). This distinct shift in the location of GFP^+ cells in the $p27^{Kip1}$ treated brains suggested that $p27^{Kip1}$ promotes NPCs to exit the cell cycle and migrate to the CP, similar to Mcl-1 gain-of-function (Figure 3.1). So, I next asked whether there is a difference in NPC differentiation within the $p27^{Kip1}$ treated brains when compared to control. Tbr1 immunohistochemistry was performed 48 hours post electroporation on control and $p27^{Kip1}$ transfected brain sections to label the differentiated neurons. In control brains 11±2% of transfected cells were also $Tbr1^+$. In contrast, 26±2% of transfected cells were also $Tbr1^+$ in $p27^{Kip1}$ treated brains (Figure 3.9B). The 2-fold increase in differentiated neurons within $p27^{Kip1}$ electroporated brains suggests that $p27^{Kip1}$ promotes NPC neurogenesis similar to Mcl-1 gain-of-function (Figure 3.3).

Figure 3.9: $p27^{Kip1}$ affects NPC differentiation similar to Mcl-1 *in vivo*.

A – Quantification of the percent GFP^+ cells located in VZ, SVZ and CP within control (Ctl) and $p27^{Kip1}$ treated brains. GFP^+ cells were counted in 3 representative sections per embryo (n=4/treatment). Mean cell counts were analyzed by t-test with statistical significance assessed at *$p<0.05$. Graphs represent mean±SEM.

B – Quantification of the percent double labeled GFP^+ and $Tbr1^+$ cells in control (Ctl) and $p27^{Kip1}$ electroporated brains. GFP^+ cells were counted in 3 representative sections per embryo (n=4/treatment). Mean cell counts were analyzed by t-test with statistical significance assessed at *$p<0.05$. Graphs represent means ±SEM.

A

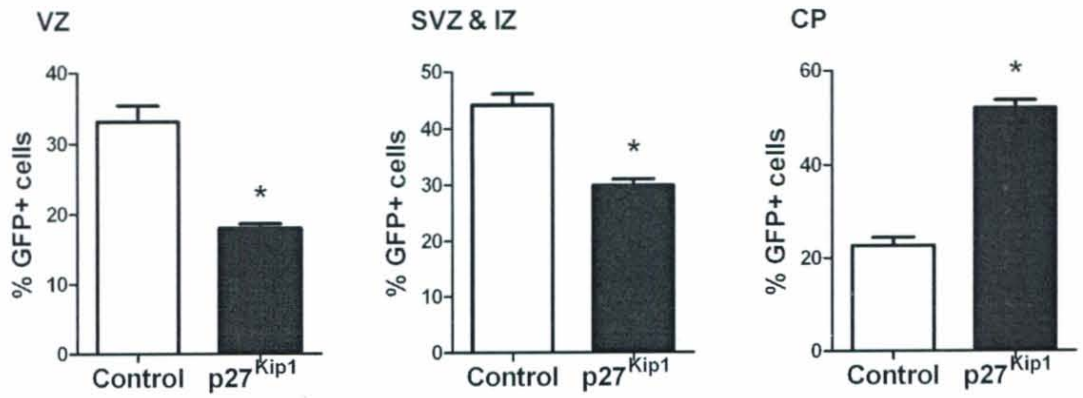
VZ
SVZ & IZ
CP
% GFP+ cells
40
30
20
10
0
50
60
*
Control
p27Kip1

B

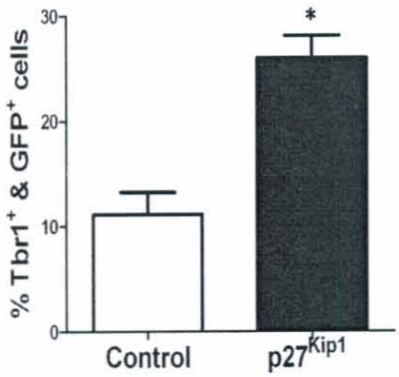
% Tbr1+ & GFP+ cells
30
20
10
0
*
Control
p27Kip1

3.10 $p27^{Kip1}$ and Mcl-1 regulate NPC proliferation at the same rate *in vitro*

The *in vivo* data revealed that $p27^{Kip1}$ promotes differentiation of NPCs similar to Mcl-1 (Figure 3.1, 3.3, 3.9). So, I next investigated whether $p27^{Kip1}$ affect NPC proliferation similar to Mcl-1, when cultured under proliferating conditions *in vitro* (Figure 3.6). I cultured E13 NPCs and transfected them with control, mt Mcl-1 or $p27^{Kip1}$ plasmids. To maintain transfected NPCs in a proliferative state, I cultured cells in high concentration of FGF-2, a potent growth factor that promotes NPC proliferation (Sosunov and Chelyshev Iu, 2002).

The cultures were fixed at 24, 48 and 72 hours post-electroporation and immunocytochemistry for PCNA was performed to label the proliferating cells The $PCNA^+$ transfected cells were quantified to assess proliferation. 24 hours post transfection, 86±1% of GFP^+ cells were also $PCNA^+$ in the control cultures, 72±1% of GFP^+ cells were $PCNA^+$ in the mt Mcl-1 treated cultures and 71±1% GFP^+ cells were $PCNA^+$ in the $p27^{Kip1}$ treated cultures. 48 hours post transfection, 80±1% of GFP^+ cells were also $PCNA^+$ in control cultures, 70±1% of GFP^+ cells were $PCNA^+$ in mt Mcl-1 treated cultures and 68±1% of GFP+ cells were $PCNA^+$ in the $p27^{Kip1}$ treated cultures. The greatest difference was observed at 72 hours post transfection when, 57±9% of transfected cells were also $PCNA^+$ in control cultures, whereas only 36±2% of transfected cells were $PCNA^+$ in mt Mcl-1 treated cultures and 35±1% of transfected cells were $PCNA^+$ in the $p27^{Kip1}$ treated cultures (Figure 3.6). The significant reduction in proliferation upon either Mcl-1 or $p27^{Kip1}$ overexpression at 24, 48 and 72 hours post transfection supports our *in vitro* findings that Mcl-1 and $p27^{Kip1}$ reduce NPC proliferation at similar rates. This suggests that both Mcl-1 and $p27^{Kip1}$ may be part of the same mechanism that promotes NPC cell cycle exit.

Figure 3.10: $p27^{Kip1}$ and Mcl-1 reduces NPC proliferation at similar rates *in vitro*.

Quantification of the percent of GFP^+ cells that are also $PCNA^+$ in control (Ctl), mt Mcl-1 and $P27^{Kip1}$ transfected NPC cultures. Cultures were fixed at 24, 48 or 72 hours post transfection. Proliferation was assessed with PCNA immunocytochemistry (n=3/treatment). Mean cell counts were analyzed by 1-way ANOVA followed by Tukey's post hoc analysis with statistical significance assessed at *$p<0.01$. Graphs represent means ±SEM.

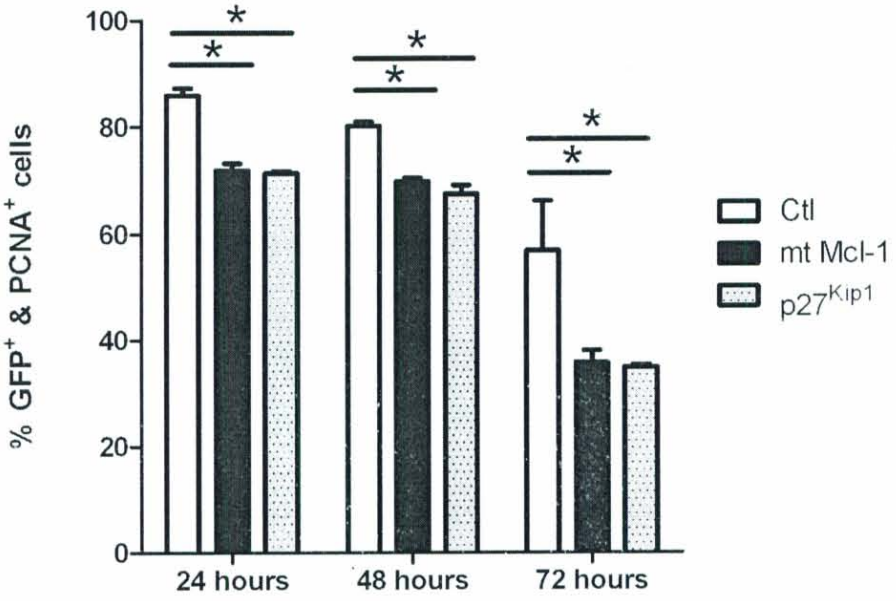
% GFP+ & PCNA+ cells
100
80
60
40
20
0
*
*
*
*
*
*
24 hours
48 hours
72 hours
Ctl
mt Mcl-1
p27Kip1

3.11 Mcl-1 regulates NPC proliferation through $p27^{Kip1}$ activity

I next asked whether $p27^{Kip1}$ is required for Mcl-1 to promote NPC cell cycle exit. So I assessed the effect of Mcl-1 on NPC proliferation in the absence of $p27^{Kip1}$. NPCs were cultured from $p27^{Kip1}$ null embryos (-/-) and wildtype littermate controls (+/+) at E13, transfected with control (Ctl) or mt Mcl-1 plasmids and plated at clonal density. NPCs were maintained in proliferating media with high concentration of FGF-2. The cultures received a BrdU pulse 2 hours before fixation at 24, 48 and 72 hours following transfection of NPCs. BrdU labels the cells in S-phase. Immunocytochemistry for BrdU was carried out and the $BrdU^+$ transfected cells were quantified. Cells double labeled for both GFP and BrdU were expressed as a percentage of total GFP^+ cells to assess the proliferating status.

Mcl-1 gain-of-function reduced proliferation of wildtype NPCs (wt : mt Mcl-1) by 2-fold when compared to control transfected NPCs (wt : Ctl) (Figure 3.11), both at 24 hours and 48 hours post transfection. This supports my previous data, which demonstrated that Mcl-1 promotes NPC cell cycle exit in a cell autonomous manner (Figure 3.6). In contrast, overexpression of mt Mcl-1 in the $p27^{Kip1}$-null NPCs did not reduce proliferation at any time points studied (Figure 3.11). Regardless of whether $p27^{Kip1}$-null NPCs were transfected with control or mt Mcl-1 plasmids, they remained highly proliferating even after 72 hours post transfection ($*p<0.001$ for all time points). These results indicate that Mcl-1 does not affect NPC proliferation in absence of $p27^{Kip1}$, suggesting that Mcl-1 promotes NPC cell cycle exit through $p27^{Kip1}$ activity.

Figure 3.11: Proliferation is not affected by Mcl-1 in $p27^{Kip1}$ null NPCs.

A – Representative photomicrographs of wildtype (wt) or $p27^{Kip1-/-}$ cultures transfected with either Ctl or mt Mcl-1 plasmids. Panels show GFP^+ cells, $BrdU^+$ cells, Hoechst nuclear staining and merged images.

B – Quantification of the percent of GFP^+ cells that are also $BrdU^+$ in control (Ctl) and mt Mcl-1 transfected NPC cultures. NPCs were generated from $p27^{Kip1}$ null embryos ($p27^{Kip1-/-}$) and wildtype littermate controls (wt) and proliferation was assessed at 24, 48 and 72 hours post transfection (n=3/genotype). Mean cell counts were analyzed by 2-way ANOVA followed by Tukey's post hoc analysis with statistical significance assessed at $*p<0.01$ or $**p<0.001$. Graphs represent means ±SEM.

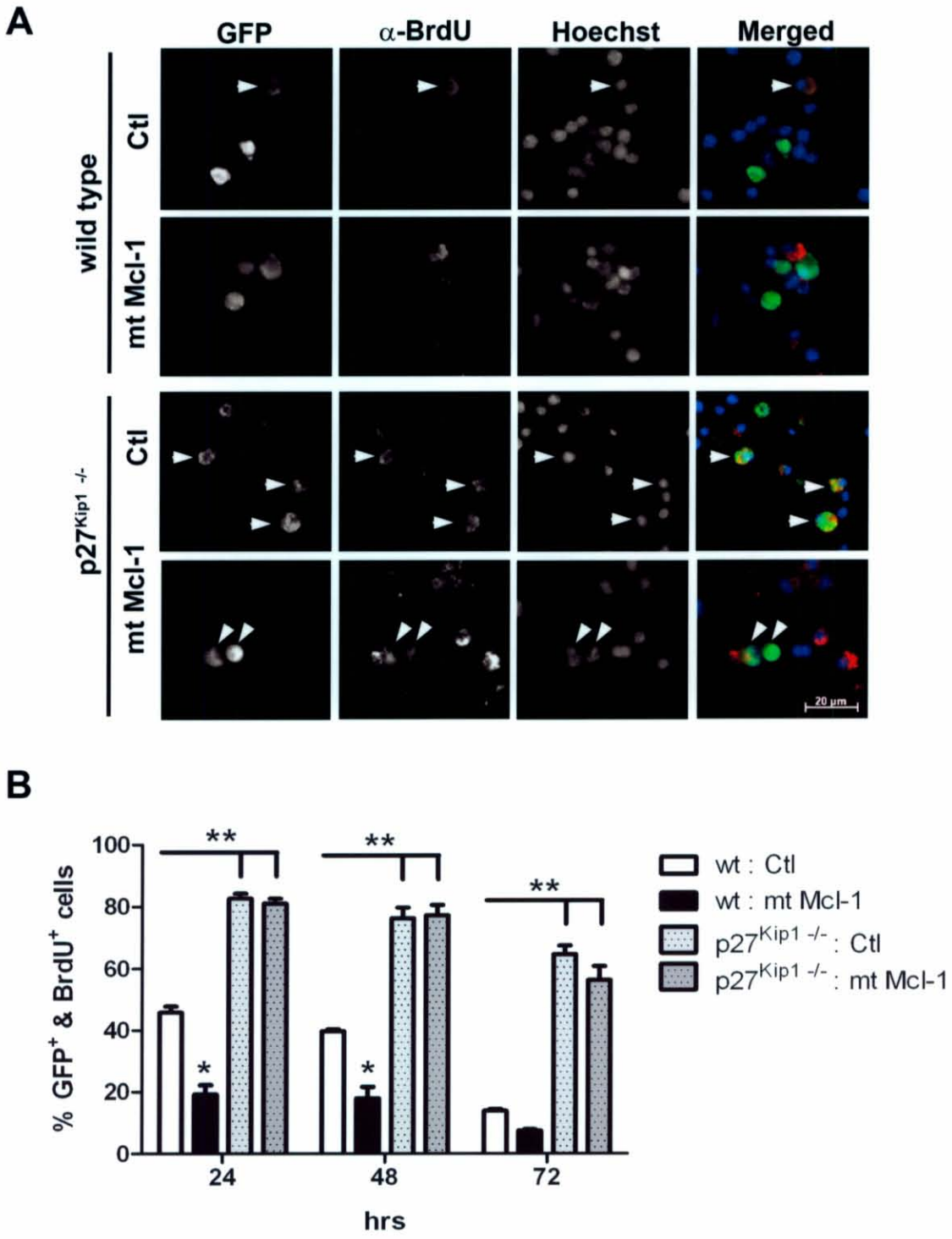
A
GFP
α-BrdU
Hoechst
Merged
wild type
Ctl
mt Mcl-1
p27Kip1 -/-
Ctl
mt Mcl-1
20 μm
B
% GFP+ & BrdU+ cells
100
80
60
40
20
0
**
**
**
*
*
24
48
72
hrs
wt : Ctl
wt : mt Mcl-1
p27Kip1 -/- : Ctl
p27Kip1 -/- : mt Mcl-1

Chapter 4

Discussion

4.1 Mcl-1 promotes cell cycle exit of embryonic NPCs

Mcl-1 is a critical survival factor among stem cell populations. It is required for the survival of hematopoietic stem cells and the development and survival of B and T lymphocytes (Opferman et al., 2005). Mcl-1 has also been identified as a survival factor for hepatic and epidermal proliferating precursors (Sitailo et al., 2009, Vick et al., 2009). Similarly, conditional knockout of Mcl-1 in NPCs causes widespread apoptosis among NPCs, migrating neuroblasts and immature neurons (Arbour et al., 2008). Therefore, not only is Mcl-1 critical for the survival of different precursor populations, but also crucial for survival during the time of cell differentiation.

Mcl-1 was first discovered as a gene that is upregulated during induced differentiation of human myeloblastic leukemia cells (Kozopas et al., 1993). Germline knockout of Mcl-1 results in peri-implantation lethality in mice at E3.5 due to defects in trophectoderm formation, suggesting that Mcl-1 may have other roles than cell survival (Rinkenberger et al., 2000). However, the only evidence of Mcl-1 affecting cell cycle regulation comes from a limited number of *in vitro* studies involving forced expression of Mcl-1 in cell lines (Fujise et al., 2000, Jamil et al., 2005). At present, there is no physiological *in vivo* evidence of Mcl-1 regulating cell cycle progression.

I investigated the role of Mcl-1 on NPC cell cycle since it is the only Bcl-2 family member that is required for the survival of embryonic NPCs and appears to be a critical survival factor during the time of NPC differentiation (Arbour et al., 2008). From my studies, I have demonstrated a

novel role of Mcl-1 using an *in vivo* model. I have shown that through a cell autonomous mechanism, Mcl-1 promotes cell cycle exit and differentiation of NPCs. Cells that prematurely exit the cell cycle upon Mcl-1 overexpression form neurons in the deeper cortical layers, confirming their earlier birthdate. However, based on these studies, no functional differences can be drawn between cell cycle exit and differentiation of NPCs. I have assessed neuronal differentiation using Tbr1 expression, a marker for newborn neurons, and separately assessed cell cycle exit using BrdU birthdating. Taken together, I have demonstrated that Mcl-1 affects both aspects of NPC cell cycle – it promotes cell cycle exit and differentiation of NPCs.

I have characterized Mcl-1 as a mediator of NPC cell cycle exit based on gain-of-function experiments. The main challenge in the Mcl-1 loss-of-function model comes from the high level of apoptosis in the absence of Mcl-1. Nonetheless, complementing data from loss-of-function experiments will further support a role for Mcl-1 as a promoter of NPC cell cycle exit. This can be performed using apoptotic inhibitors in proliferation or differentiation assays on Mcl-1 CKO NPCs. Since activation of executioner caspases like Caspase-3 is required for completion of apoptosis, caspase-3 inhibitors like z-Asp-Glu-Val-Asp-fluoromethyl ketone (z-DEVD-fmk) can be used (Liu et al., 1998, Taylor et al., 2008).

4.2 Mcl-1 directly interacts with cell cycle regulators in NPCs

Previous evidence of Mcl-1 interacting with cell cycle regulators comes either from forced expression of Mcl-1 in cell lines or from studies inducing cell cycle arrest. Since Mcl-1 has been shown to interact with PCNA and Cdk1-Cyclin B1 under such conditions (Fujise et al., 2000, Jamil et al., 2005, Harley et al., 2010), I investigated whether Mcl-1 binds to either PCNA or

Cdk1-Cyclin B1 in NPCs. My results show that Mcl-1 directly binds to both PCNA and Cdk1-Cyclin B1 complex in NPCs. Immunoprecipitation results however, also revealed that Mcl-1 gain-of-function sequestered more Cdk1-Cyclin B1 complex, whereas there was no difference with PCNA. It remains to be determined, whether this difference is responsible for the NPC cell cycle exit.

Association between Cdk1-Cyclin B1 and Mcl-1 is of particular interest because: (1) expression of Mcl-1 protein level peaks at mitosis (Harley et al., 2010); (2) transition to mitosis is regulated by Cdk1-Cyclin B1 activity (Nurse, 1994); and (3) as I have shown, overexpression of Mcl-1 sequesters more of the cell's Cdk1-Cyclin B1 complexes. Cdk1-Cyclin B1 promotes cell cycle progression, whereas Mcl-1 promotes cell cycle exit. Therefore, increased sequestering of Cdk1-Cyclin B1 by Mcl-1 may represent a way by which Mcl-1 alters Cdk1-Cyclin B1 activity during mitosis promoting cell cycle exit.

4.3 Cdk inhibitor $p27^{Kip1}$ is required for Mcl-1 mediated cell cycle exit

The Cdk inhibitor $p27^{Kip1}$ has been shown to promote cell cycle arrest of NPCs during embryogenesis (Fero et al., 1996, Kiyokawa et al., 1996, Nakayama et al., 1996, Carruthers et al., 2003). Overexpression of $p27^{Kip1}$ in cortical progenitors promotes premature cell cycle exit and a reduction of upper layer neurons, which are born later (Tarui et al., 2005). In contrast, $p27^{Kip1}$-null mice demonstrate continued proliferation of NPCs and a decrease in neuronal production during mid-corticogenesis. This results in an increase in production of late-born neurons and subsequent enlargement of upper cortical layers (Goto et al., 2004).

I have demonstrated that changes in Mcl-1 expression results in concomitant changes in $p27^{Kip1}$ protein level. In addition, overexpression of $p27^{Kip1}$ mirrors the effects of Mcl-1 overexpression in NPCs both *in vivo* and *in vitro*. Furthermore, Mcl-1 gain-of-function fails to promote cell cycle exit in $p27^{Kip1}$-null NPCs. Taken together, I have demonstrated that Mcl-1 promotes NPC cell cycle exit through $p27^{Kip1}$ activity.

How changes in Mcl-1 expression cause concomitant changes in $p27^{Kip1}$ protein remains to be determined. Since phosphorylation of $p27^{Kip1}$ protein regulates its turnover and functional role in promoting cell cycle exit (Pagano et al., 1995, Loda et al., 1997), it is possible that Mcl-1 gain-of-function or loss-of-function changes the phosphorylation status of $p27^{Kip1}$ protein. This will be an area for future investigation.

4.4 Future Directions

I have demonstrated a novel function of anti-apoptotic Mcl-1 in NPCs. Apart from its critical role in survival, Mcl-1 promotes cell cycle exit of NPCs in a cell autonomous manner and promotes their differentiation. The cell cycle exit is mediated through Cdk inhibitor $p27^{Kip1}$, however any direct regulation of $p27^{Kip1}$ protein by Mcl-1 is still unknown. Mcl-1 also differentially binds to Cdk1-Cyclin B1 when more abundant, but whether this association promotes NPC cell cycle exit also remains to be determined.

4.4.1 How do changes in Mcl-1 expression affect $p27^{Kip1}$ protein?

Functional properties of $p27^{Kip1}$ protein are regulated by phosphorylation. In particular, phosphorylation of S10 and T187 residue is implicated in promoting neuronal differentiation of neural stem cells and migration of differentiating neuroblasts (Zheng et al., 2010). Since Mcl-1 gain-of-function sequesters more Cdk1-Cyclin B1 complex and also increases $p27^{Kip1}$ protein expression, it is possible that the two processes are related and together promote cell cycle exit and differentiation of NPCs. Cdk/Cyclin complexes phosphorylate $p27^{Kip1}$ on T187. One possibility is that the association with Mcl-1 affects the kinase activity of Cdk1-Cyclin B1 to promote $p27^{Kip1}$ phosphorylation on T187, and in doing so promotes its neurogenic function.

To address whether Mcl-1 affects $p27^{Kip1}$ phosphorylation, both gain-of-function and loss-of-function strategies can be implemented. Specifically for Mcl-1 gain-of-function, NPCs can be transfected with either control or mt Mcl-1 plasmids followed by quantification of T187 phosphorylated $p27^{Kip1}$ in the two cultures. However, a low transfection efficiency of primary cultures makes this challenging. Techniques like western analysis cannot separate the transfected NPCs from the heterogeneous culture, and thus may fail to detect changes in $p27^{Kip1}$ phosphorylation at specific sites with Mcl-1 overexpression. Performing a flow cytometric analysis will overcome this problem. This way changes in the phosphorylation status of $p27^{Kip1}$ will only be recorded from GFP^{+} transfected cells using antibodies specific to $p27^{Kip1}$-phosphorylated residues. For the Mcl-1 loss-of-function model, it will be less challenging since Mcl-1 is conditionally knocked out from all NPCs (Arbour et al., 2008). If Mcl-1 does promote phosphorylation on T187 of $p27^{Kip1}$, I expect an increase in T187 phosphorylated $p27^{Kip1}$ protein

in mt Mcl-1 transfected NPCs and alternately, a reduction in phosphorylated $p27^{Kip1}$ protein in Mcl-1 CKO NPCs. Therefore, it is possible to analyze changes in the phosphorylation status of $p27^{Kip1}$ with changes in Mcl-1 expression, which will give a more complete picture about the mechanism of NPC cell cycle exit.

4.4.2 Is the association between Mcl-1 and Cdk1-Cyclin B1 required for NPC cell cycle exit?

To determine whether sequestering of Cdk1-Cyclin B1 by Mcl-1 promotes NPC cell cycle exit, it is important to identify the putative binding site(s) on Mcl-1 that are required for interacting with Cdk1-Cyclin B1. Once the site(s) are identified, site-specific Mcl-1 mutant constructs can be generated that abrogate its interaction with Cdk1-Cylin B1. Using site-specific mutant constructs, the dual roles in cell cycle progression and cell survival have been demonstrated to be functionally separate in some Bcl-2 family members (Huang et al., 1997). This model can be replicated and proliferation assays can be performed on NPCs transfected with Mcl-1 mutant constructs. This will demonstrate whether the association between Mcl-1 and Cdk1-Cyclin B1 is required for cell cycle exit. To further determine whether $p27^{Kip1}$ protein phosphorylation depends on this interaction, NPCs can be transfected with Mcl-1 mutant constructs that are unable to interact with Cdk1-Cyclin B1 and then the phosphorylation status of $p27^{Kip1}$ can be detected via flow cytometry. If the interaction between Mcl-1 and Cdk1-Cyclin B1 is required for promoting $p27^{Kip1}$ phosphorylation, attenuating this interaction will show no alterations in the phosphorylation status of $p27^{Kip1}$.

Increased association between Mcl-1 and Cdk1-Cyclin B1 may also represent a $p27^{Kip1}$

independent pathway for promoting cell cycle exit of NPCs. Cdk1-Cyclin B1 phosphorylates transcription factor N-myc on S54 and promotes its degradation by GSK-3β in NPCs (Sjostrom et al., 2005). N-myc is a downstream effector of Sonic Hedgehog (Shh) signaling that promotes proliferation of NPCs (Kenney et al., 2003). During NPC mitosis, Cdk1-Cyclin B1 phosphorylates N-myc and its degradation allows cell cycle exit and differentiation (Sjostrom et al., 2005). If increased association with Mcl-1 promotes the kinase activity of Cdk1-Cyclin B1, it may result in enhanced N-myc phosphorylation and degradation. This may also represent a mechanism by which Mcl-1 promotes NPC cycle exit and differentiation – by affecting Shh signaling. To test this, one needs to examine whether Mcl-1 gain-of-function affects N-myc phosphorylation. Furthermore, to test whether the association between Mcl-1 and Cdk1-Cyclin B1 promotes N-myc phosphorylation, NPCs can be transfected with Mcl-1 mutant constructs that are unable to associate with Cdk1-Cyclin B1 and assayed for changes in N-myc phosphorylation.

4.4.3 Does Mcl-1 affect Rb/E2F pathway to promote cell cycle exit of NPCs?

Rb/E2F activity plays a pivotal role in regulating cell cycle progression by controlling transcription of target genes (Polager and Ginsberg, 2008). During the G1 phase of the cell cycle, activity of G1 Cdks-cyclins promotes hyperphosphorylation of Rb and prevents its binding with E2Fs. Once hyperphosphorylated, Rb releases the E2F transcription factors (E2F-1, 2, 3), which are the activators of gene transcription essential for the G1 to S phase transition and commitment to mitosis (Dyson, 1998, Nevins, 1998). Since the activity of G1 Cdks-cyclins is inhibited by $p27^{Kip1}$, increased $p27^{Kip1}$ should result in hypophosphorylated Rb that is bound to E2F transcription factors, blocking cell cycle entry. Mcl-1 overexpression may therefore result in

greater association between Rb and E2Fs, through an increase in $p27^{Kip1}$. In contrast, Mcl-1 loss-of-function results in a concomitant reduction in $p27^{Kip1}$ and is likely to reflect Rb hyperphosphorylation, releasing E2F transcription factors to activate gene transcription required for cell cycle entry. This can be tested via an electromobility shift assay, which detects both the levels of free E2F proteins and E2F proteins bound to Rb. It is thus possible to detect how the Rb/E2F interaction is altered in both Mcl-1 gain-of-function and loss-of-function strategies.

The main findings and the continued hypothesis of how Mcl-1 promotes cell cycle exit of NPCs are illustrated in Figure 4.1.

Figure 4.1: Summary & the continued hypothesis of how Mcl-1 regulate cell cycle exit of NPCs.

A – In the Mcl-1 gain-of-function model, there is greater association between Mcl-1 and Cdk1-Cyclin B1. Although it remains to be determined whether this association regulates $p27^{Kip1}$ level, Mcl-1 overexpression also causes an increase in $p27^{Kip1}$. This inhibits the G1 Cdks-Cyclins responsible for phosphorylating Rb. Hence Rb remains bound to E2F transcription factors, blocking the transcription of genes necessary for progressing into G1. The G1/S block prevents cell cycle re-entry leading to cell cycle exit.

B – In the Mcl-1 loss-of-function model there is a concomitant reduction in $p27^{Kip1}$. The reduction in $p27^{Kip1}$ allows the G1 Cdks-Cyclins to hyperphosphorylate pRb. This frees E2F transcription factors to promote gene transcription required for cell cycle entry.

The solid lines represent established links in the mechanism and the dotted lines represent a hypothesized/potential pathway.

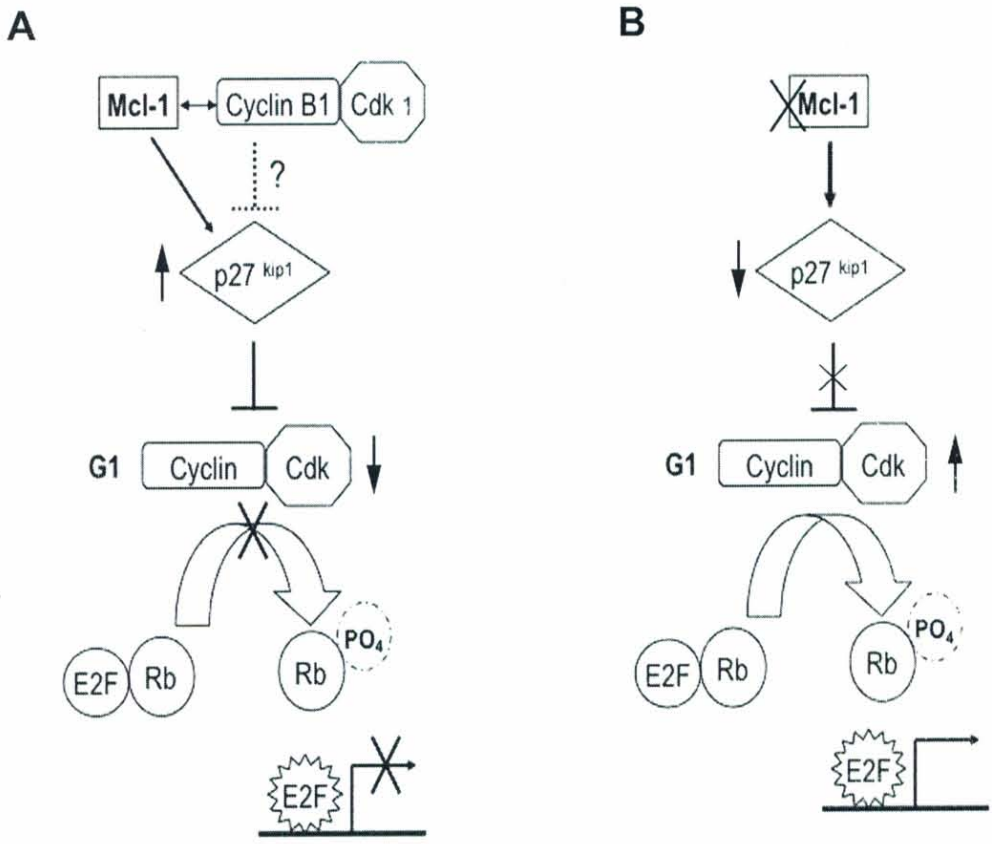
A
Mcl-1
Cyclin B1
Cdk 1
?
p27 kip1
G1
Cyclin
Cdk
E2F
Rb
Rb
PO4
E2F
B
Mcl-1
p27 kip1
G1
Cyclin
Cdk
E2F
Rb
Rb
PO4
E2F

4.4.4 Does Mcl-1 preferentially promote neuronal differentiation?

The novelty of my project arises from the discovery that Mcl-1, a critical survival factor of NPCs, also promotes cell cycle exit and differentiation of NPCs. Although I have demonstrated that Mcl-1 gain-of-function promotes neuronal differentiation of NPCs *in vivo*, it remains to be determined if Mcl-1 preferentially promotes neuronal differentiation over glial differentiation. This can be achieved *in vitro* by Mcl-1 gain-of-function in NPCs and inducing differentiation. Since NPCs are capable of differentiating into both neurons and glia, from the differentiating cultures, the percent-transfected cells that express glial markers can be compared to the percent-transfected cells expressing neuronal markers. To further demonstrate that endogenous Mcl-1 has a crucial role in neurogenesis, a differentiation assay can also be used to assess the effects of Mcl-1 loss-of-function on neuronal differentiation using Mcl-1 CKO NPCs. However, NPCs undergo apoptosis in absence of Mcl-1. This prevents assessing differentiation of NPCs since many of them will die during the experimental procedure. Therefore, the differentiation assay should be performed in the presence of an apoptotic blocker, like Caspase-3 inhibitor z-DEVD to prevent NPC apoptosis (Liu et al., 1998).

If Mcl-1 preferentially promotes neuronal differentiation over glial differentiation, the implications can be extraordinary in the field of regenerative medicine to treat neurodegenerative conditions. Although glial dysfunction is also observed in many neurodegenerative conditions, the main challenge in the aging brain comes from the severe reduction in the number of neural progenitors as well as their differentiating potential (Ahlenius et al., 2009). Regardless of whether it is through manipulation of endogenous neural stem cells or through stem cell transplants, additional key challenges in neural regeneration come from poor survival rate of NPCs and their failure to differentiate to neurons (Arvidsson et al., 2002, Parent, 2003, Haas et al., 2005, Hsu et

al., 2007). If Mcl-1 preferentially promotes neuronal differentiation, it will reflect a potential therapeutic strategy that will successfully promote NPC survival while facilitating neuronal differentiation.

4.5 Conclusions

Survival and differentiation of NPCs are key regulatory aspects of mammalian nervous system development. Although there have been suggestions that these processes are interrelated, the molecular mechanism behind this claim is still undefined. I have shown that Mcl-1, which is essential for the survival of NPCs, also causes premature terminal mitosis in NPCs. Mcl-1 promotes cell cycle exit and differentiation of NPCs into neurons of the deeper cortical layers and this is mediated through Cdk inhibitor $p27^{Kip1}$ activity. Like its pro-survival role (Arbour et al., 2008), the effect of Mcl-1 on NPC cell cycle is also mediated in a cell autonomous manner. This provides new insights into how survival and differentiation of NPCs may be related during brain development.

Appendices

Appendix I – Stem Cell Media (SCM)

DMEM/F12 (Gibco, 911330),

5.85 mg/mL D-glucose (Sigma, G7528),

1.95 mM L-glutamine (Sigma, 25030-081),

48.7 units/mL penicillin-streptomycin (Invitrogen, 15140-122),

24.4 μg/mL insulin (Sigma, I-5500),

97.4 μg/mL apotransferrin (Sigma, T4382),

0.0194 nM progesterone (Sigma, P8783),

9.36 μg/mL putrescine (Sigma, P5780),

2.92 nM selenium (Sigma, S5290),

12.1 ng/mL fungizone (Gibco, 15290-018),

1.95 μg/mL heparin (Sigma, H3149),

0.195 μg/mL FGF-2 (Sigma, F0291).

Appendix II – pCIG2 expression vector map

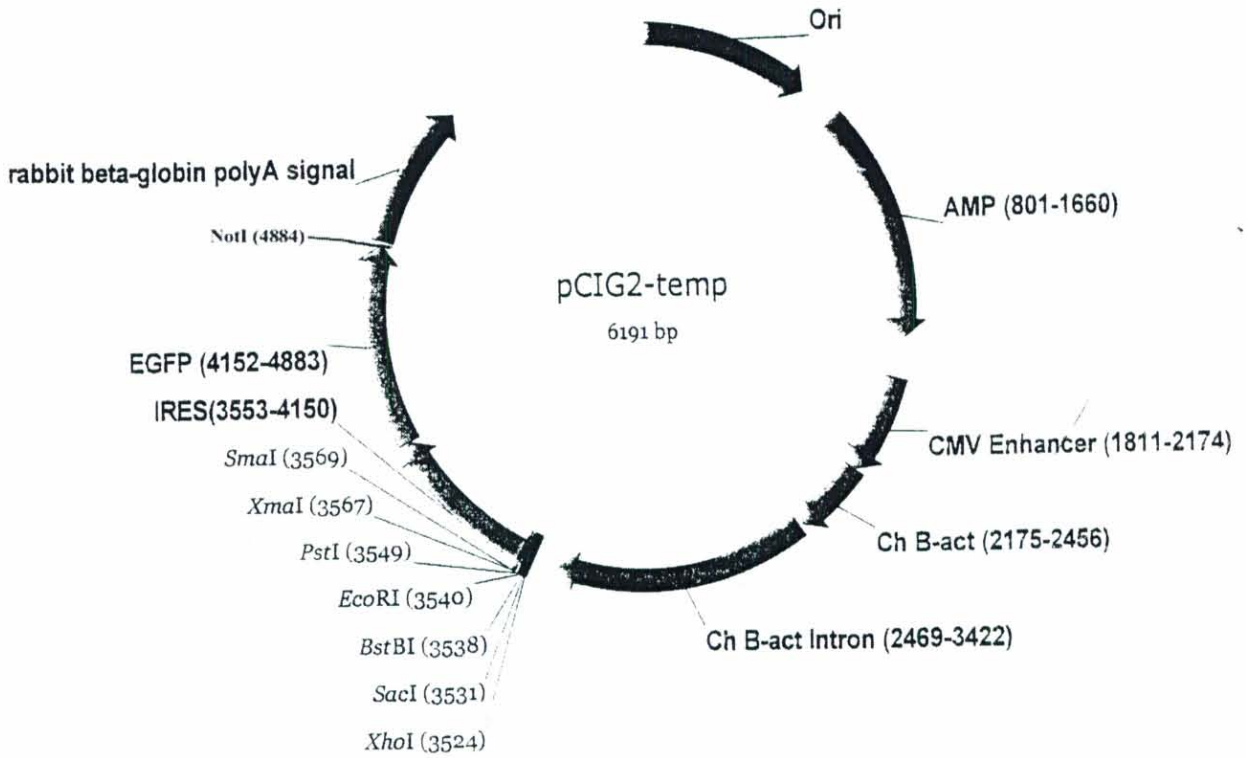

Appendix III – pCIG2 mt Mcl-1 vector map

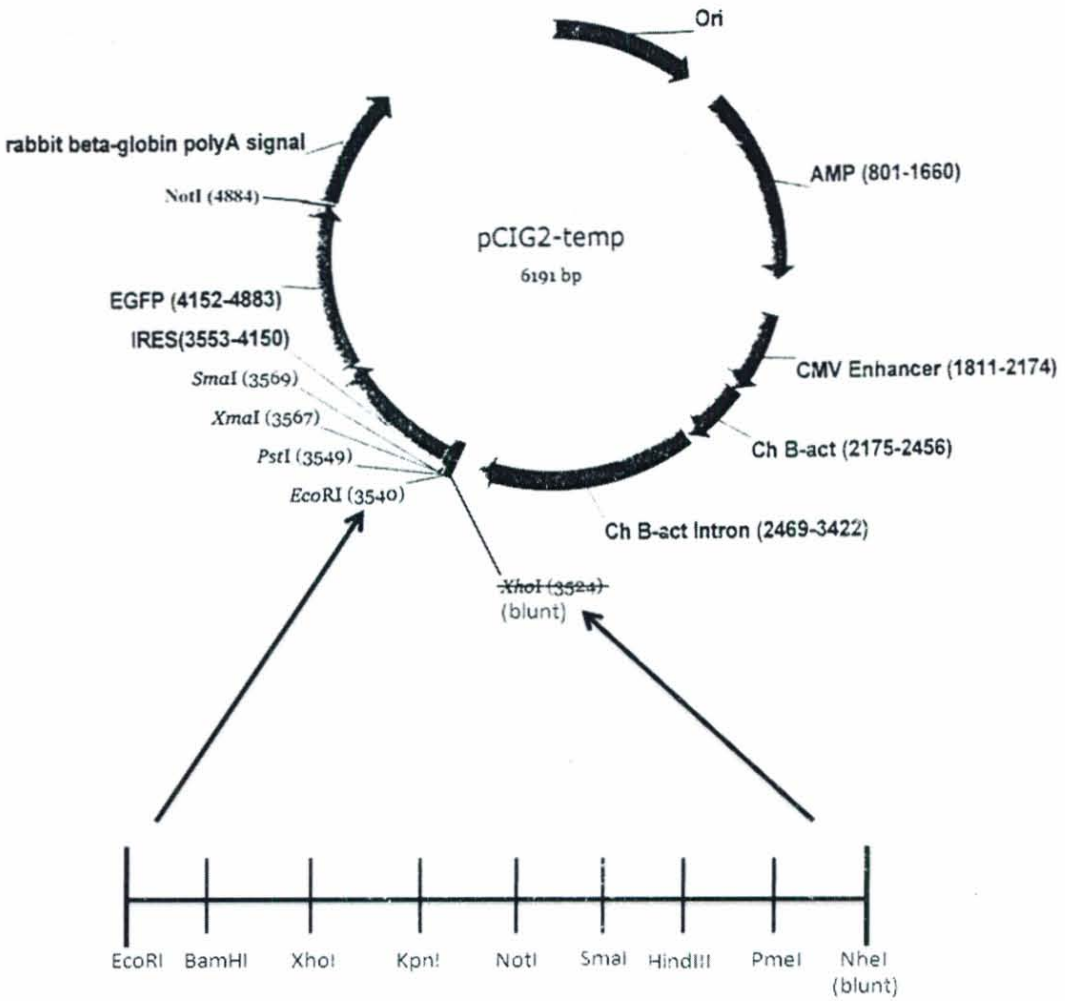

Appendix IV – pCIG2 $p27^{Kip1}$ vector map

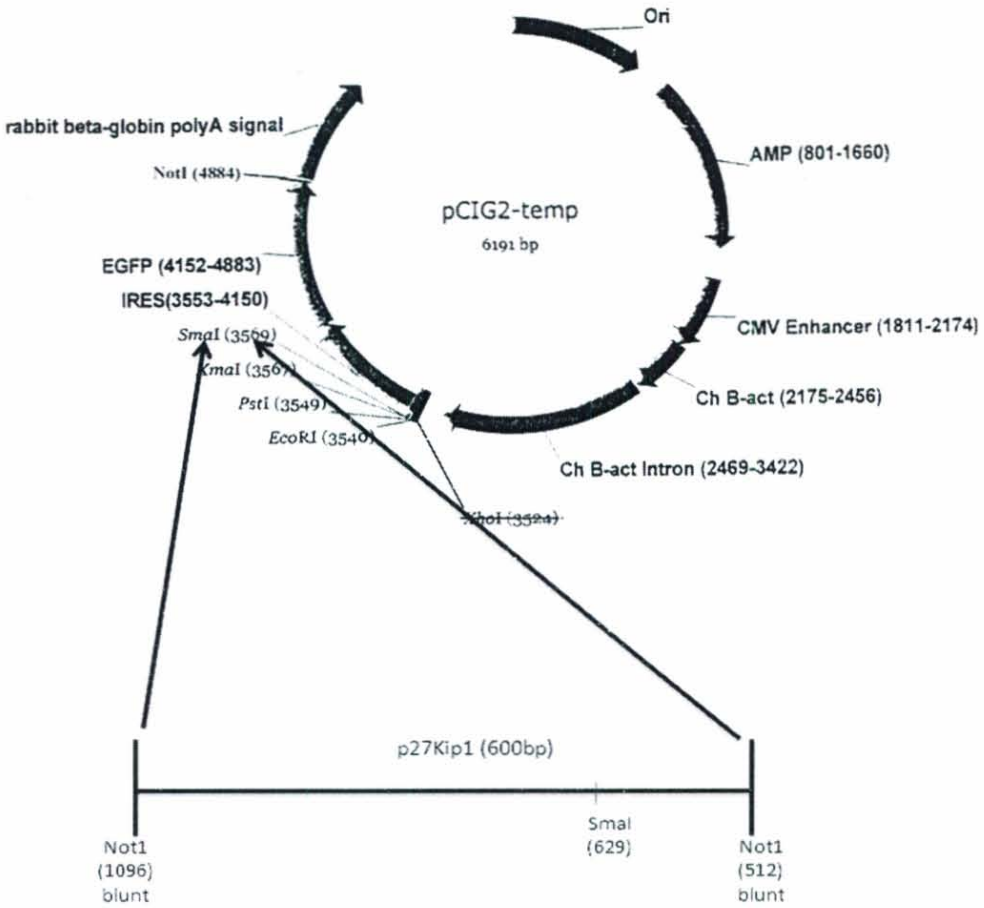

Appendix V – List of Antibodies

Antibodies	Source	Concentration for Western Blot	Concentration for Immunohistochemistry
Mcl-1	Rockland - 600401394	1:3000	1:200
Proliferating cell nuclear antigen (PCNA)	Vector Labs - VP-P980	(1:500)	(1:300)
Cdk1	Santa Cruz - SC53219	(1:500)	-
Cyclin B1	Santa Cruz - SC752	(1:500)	-
$p27^{kip1}$	BD Biosciences - 554069	(1:500)	-
β actin	Sigma - A5316-2mL	(1:3000)	-
T-box brain 1 (Tbr1)	Abcam - 31940	-	(1:500)
Cut-like transcription factor (Cux1)	Santa Cruz - SC13024	-	(1:300)
Bromodeoxyuridine (BrdU)	BD Biosciences - 347580	-	(1:100)

Appendix VI – Average number of GFP^+ cells detected per experiment for each treatment group

Experiment	No. of GFP^+ cells in Ctl treated samples	No. of GFP^+ cells in mt Mcl-1 treated samples	No. of GFP^+ cells in $p27^{Kip1}$ treated samples
Location of GFP^+ cells 48 hrs post electroporation (Figure 3.1)	109	117	-
% GFP^+ & $PCNA^+$ cells 48 hrs post electroporation (Figure 3.2)	90	65	-
% GFP^+ & $Tbr1^+$ cells 48 hrs post electroporation (Figure 3.3)	130	170	-
% GFP^+ & $BrdU^+$ cells 5 days post electroporation (Figure 3.4)	200	170	-
Location GFP^+ cells in 2-weeks postnatal brain (Figure 3.5)	98	81	-
% GFP^+ & $BrdU^+$ cells 24/48 hrs post transfection (Figure 3.6)	45	48	-
Location of GFP^+ cells 48 hrs post electroporation (Figure 3.9)	380	-	270
% GFP^+ & $Tbr1^+$ cells 48 hrs post electroporation (Figure 3.9)	366	-	308
% GFP^+ & $PCNA^+$ cells 24,48 and 72 hrs post transfection (Figure 3.10)	225	228	220
% GFP^+ & $BrdU^+$ cells 24/48 hrs post transfection in wt NPCs (Figure 3.11)	151	154	-
% GFP^+ & $BrdU^+$ cells 24/48 hrs post transfection in $p27^{Kip1-/-}$ NPCs (Figure 3.11)	157	156	-

References

Adams KW, Cooper GM (2007) Rapid turnover of mcl-1 couples translation to cell survival and apoptosis. J Biol Chem 282:6192-6200.

Ahlenius H, Visan V, Kokaia M, Lindvall O, Kokaia Z (2009) Neural stem and progenitor cells retain their potential for proliferation and differentiation into functional neurons despite lower number in aged brain. J Neurosci 29:4408-4419.

Alcantara S, Ruiz M, D'Arcangelo G, Ezan F, de Lecea L, Curran T, Sotelo C, Soriano E (1998) Regional and cellular patterns of reelin mRNA expression in the forebrain of the developing and adult mouse. J Neurosci 18:7779-7799.

Allsopp TE, Wyatt S, Paterson HF, Davies AM (1993) The proto-oncogene bcl-2 can selectively rescue neurotrophic factor-dependent neurons from apoptosis. Cell 73:295-307.

Anthony TE, Klein C, Fishell G, Heintz N (2004) Radial glia serve as neuronal progenitors in all regions of the central nervous system. Neuron 41:881-890.

Arbour N, Vanderluit JL, Le Grand JN, Jahani-Asl A, Ruzhynsky VA, Cheung EC, Kelly MA, MacKenzie AE, Park DS, Opferman JT, Slack RS (2008) Mcl-1 is a key regulator of apoptosis during CNS development and after DNA damage. J Neurosci 28:6068-6078.

Arvidsson A, Collin T, Kirik D, Kokaia Z, Lindvall O (2002) Neuronal replacement from endogenous precursors in the adult brain after stroke Nat Med 8:963-970.

Bacchi CE, Gown AM (1993) Detection of cell proliferation in tissue sections. Braz J Med Biol Res 26:677-687.

Bai L, Ni HM, Chen X, DiFrancesca D, Yin XM (2005) Deletion of Bid impedes cell proliferation and hepatic carcinogenesis. Am J Pathol 166:1523-1532.

Berube NG, Mangelsdorf M, Jagla M, Vanderluit J, Garrick D, Gibbons RJ, Higgs DR, Slack RS, Picketts DJ (2005) The chromatin-remodeling protein ATRX is critical for neuronal survival during corticogenesis. J Clin Invest 115:258-267.

Bingle CD, Craig RW, Swales BM, Singleton V, Zhou P, Whyte MK (2000) Exon skipping in Mcl-1 results in a bcl-2 homology domain 3 only gene product that promotes cell death. J Biol Chem 275:22136-22146.

Blaschke AJ, Staley K, Chun J (1996) Widespread programmed cell death in proliferative and postmitotic regions of the fetal cerebral cortex. Development 122:1165-1174.

Blomer U, Kafri T, Randolph-Moore L, Verma IM, Gage FH (1998) Bcl-xL protects adult septal cholinergic neurons from axotomized cell death. Proc Natl Acad Sci U S A 95:2603-2608.

Blomgren K, Leist M, Groc L (2007) Pathological apoptosis in the developing brain. Apoptosis 12:993-1010.

Brady HJ, Gil-Gomez G, Kirberg J, Berns AJ (1996) Bax alpha perturbs T cell development and affects cell cycle entry of T cells. Embo J 15:6991-7001.

Callaghan DA, Dong L, Callaghan SM, Hou YX, Dagnino L, Slack RS (1999) Neural precursor cells differentiating in the absence of Rb exhibit delayed terminal mitosis and deregulated E2F 1 and 3 activity. Dev Biol 207:257-270.

Campbell K, Gotz M (2002) Radial glia: multi-purpose cells for vertebrate brain development. Trends Neurosci 25:235-238.

Carruthers S, Mason J, Papalopulu N (2003) Depletion of the cell-cycle inhibitor p27(Xic1) impairs neuronal differentiation and increases the number of ElrC(+) progenitor cells in Xenopus tropicalis. Mech Dev 120:607-616.

Caviness VS, Jr., Nowakowski RS, Bhide PG (2009) Neocortical neurogenesis: morphogenetic gradients and beyond. Trends Neurosci 32:443-450.

Caviness VS, Jr., Takahashi T, Nowakowski RS (1999) The G1 restriction point as critical regulator of neocortical neuronogenesis. Neurochem Res 24:497-506.

Chattopadhyay A, Chiang CW, Yang E (2001) BAD/BCL-[X(L)] heterodimerization leads to bypass of G0/G1 arrest. Oncogene 20:4507-4518.

Chipuk JE, Green DR (2008) How do BCL-2 proteins induce mitochondrial outer membrane permeabilization? Trends Cell Biol 18:157-164.

Classon M, Dyson N (2001) p107 and p130: versatile proteins with interesting pockets. Exp Cell Res 264:135-147.

Craig RW (2002) MCL1 provides a window on the role of the BCL2 family in cell proliferation, differentiation and tumorigenesis. Leukemia 16:444-454.

Cuconati A, Mukherjee C, Perez D, White E (2003) DNA damage response and MCL-1 destruction initiate apoptosis in adenovirus-infected cells. Genes Dev 17:2922-2932.

Cunningham JJ, Roussel MF (2001) Cyclin-dependent kinase inhibitors in the development of the central nervous system. Cell Growth Differ 12:387-396.

D'Arcangelo G, Miao GG, Chen SC, Soares HD, Morgan JI, Curran T (1995) A protein related to extracellular matrix proteins deleted in the mouse mutant reeler. Nature 374:719-723.

Datta SR, Dudek H, Tao X, Masters S, Fu H, Gotoh Y, Greenberg ME (1997) Akt phosphorylation of BAD couples survival signals to the cell-intrinsic death machinery. Cell 91:231-241.

de la Rosa EJ, de Pablo F (2000) Cell death in early neural development: beyond the neurotrophic theory. Trends Neurosci 23:454-458.

Deckwerth TL, Elliott JL, Knudson CM, Johnson EM, Jr., Snider WD, Korsmeyer SJ (1996) BAX is required for neuronal death after trophic factor deprivation and during development. Neuron 17:401-411.

Dehay C, Kennedy H (2007) Cell-cycle control and cortical development. Nat Rev Neurosci 8:438-450.

Deng X, Mercer SE, Shah S, Ewton DZ, Friedman E (2004) The cyclin-dependent kinase inhibitor p27Kip1 is stabilized in G(0) by Mirk/dyrk1B kinase. J Biol Chem 279:22498-22504.

Deshmukh M, Johnson EM, Jr. (1998) Evidence of a novel event during neuronal death: development of competence-to-die in response to cytoplasmic cytochrome c. Neuron 21:695-705.

Ding Q, He X, Hsu JM, Xia W, Chen CT, Li LY, Lee DF, Liu JC, Zhong Q, Wang X, Hung MC (2007) Degradation of Mcl-1 by beta-TrCP mediates glycogen synthase kinase 3-induced tumor suppression and chemosensitization. Mol Cell Biol 27:4006-4017.

Doetsch F, Verdugo JM, Caille I, Alvarez-Buylla A, Chao MV, Casaccia-Bonnefil P (2002) Lack of the cell-cycle inhibitor p27Kip1 results in selective increase of transit-amplifying cells for adult neurogenesis. J Neurosci 22:2255-2264.

Dyer MA, Cepko CL (2001) p27Kip1 and p57Kip2 regulate proliferation in distinct retinal progenitor cell populations. J Neurosci 21:4259-4271.

Dyson N (1998) The regulation of E2F by pRB-family proteins. Genes Dev 12:2245-2262.

Elledge SJ, Harper JW (1994) Cdk inhibitors: on the threshold of checkpoints and development. Curr Opin Cell Biol 6:847-852.

Englund C, Fink A, Lau C, Pham D, Daza RA, Bulfone A, Kowalczyk T, Hevner RF (2005) Pax6, Tbr2, and Tbr1 are expressed sequentially by radial glia, intermediate progenitor cells, and postmitotic neurons in developing neocortex. J Neurosci 25:247-251.

Fan TJ, Han LH, Cong RS, Liang J (2005) Caspase family proteases and apoptosis. Acta Biochim Biophys Sin (Shanghai) 37:719-727.

Farlie PG, Dringen R, Rees SM, Kannourakis G, Bernard O (1995) bcl-2 transgene expression can protect neurons against developmental and induced cell death. Proc Natl Acad Sci U S A 92:4397-4401.

Ferguson KL, Vanderluit JL, Hebert JM, McIntosh WC, Tibbo E, MacLaurin JG, Park DS, Wallace VA, Vooijs M, McConnell SK, Slack RS (2002) Telencephalon-specific Rb knockouts reveal enhanced neurogenesis, survival and abnormal cortical development. Embo J 21:3337-3346.

Fero ML, Rivkin M, Tasch M, Porter P, Carow CE, Firpo E, Polyak K, Tsai LH, Broudy V, Perlmutter RM, Kaushansky K, Roberts JM (1996) A syndrome of multiorgan hyperplasia with features of gigantism, tumorigenesis, and female sterility in p27(Kip1)-deficient mice. Cell 85:733-744.

Fujise K, Zhang D, Liu J, Yeh ET (2000) Regulation of apoptosis and cell cycle progression by MCL1. Differential role of proliferating cell nuclear antigen. J Biol Chem 275:39458-39465.

Fung YK, Murphree AL, T'Ang A, Qian J, Hinrichs SH, Benedict WF (1987) Structural evidence for the authenticity of the human retinoblastoma gene. Science 236:1657-1661.

Goto T, Mitsuhashi T, Takahashi T (2004) Altered patterns of neuron production in the p27 knockout mouse. Dev Neurosci 26:208-217.

Gotz M (2003) Glial cells generate neurons--master control within CNS regions: developmental perspectives on neural stem cells. Neuroscientist 9:379-397.

Gotz M, Barde YA (2005) Radial glial cells defined and major intermediates between embryonic stem cells and CNS neurons. Neuron 46:369-372.

Gotz M, Huttner WB (2005) The cell biology of neurogenesis. Nat Rev Mol Cell Biol 6:777-788.

Greider C, Chattopadhyay A, Parkhurst C, Yang E (2002) BCL-x(L) and BCL2 delay Myc-induced cell cycle entry through elevation of p27 and inhibition of G1 cyclin-dependent kinases. Oncogene 21:7765-7775.

Haas S, Weidner N, Winkler J (2005) Adult stem cell therapy in stroke. Curr Opin Neurol 18:59-64.

Harley ME, Allan LA, Sanderson HS, Clarke PR (2010) Phosphorylation of Mcl-1 by CDK1-cyclin B1 initiates its Cdc20-dependent destruction during mitotic arrest. Embo J 29:2407-2420.

Hartfuss E, Galli R, Heins N, Gotz M (2001) Characterization of CNS precursor subtypes and radial glia. Dev Biol 229:15-30.

Haubensak W, Attardo A, Denk W, Huttner WB (2004) Neurons arise in the basal neuroepithelium of the early mammalian telencephalon: a major site of neurogenesis. Proc Natl Acad Sci U S A 101:3196-3201.

Haydar TF, Kuan CY, Flavell RA, Rakic P (1999) The role of cell death in regulating the size and shape of the mammalian forebrain. Cereb Cortex 9:621-626.

Hevner RF, Hodge RD, Daza RA, Englund C (2006) Transcription factors in glutamatergic neurogenesis: conserved programs in neocortex, cerebellum, and adult hippocampus. Neurosci Res 55:223-233.

Hirotsune S, Takahara T, Sasaki N, Hirose K, Yoshiki A, Ohashi T, Kusakabe M, Murakami Y, Muramatsu M, Watanabe S, et al. (1995) The reeler gene encodes a protein with an EGF-like motif expressed by pioneer neurons. Nat Genet 10:77-83.

Hsu YC, Lee DC, Chiu IM (2007) Neural stem cells, neural progenitors, and neurotrophic factors. Cell Transplant 16:133-150.

Huang DC, O'Reilly LA, Strasser A, Cory S (1997) The anti-apoptosis function of Bcl-2 can be genetically separated from its inhibitory effect on cell cycle entry. Embo J 16:4628-4638.

Huttner WB, Kosodo Y (2005) Symmetric versus asymmetric cell division during neurogenesis in the developing vertebrate central nervous system. Curr Opin Cell Biol 17:648-657.

Jamil S, Sobouti R, Hojabrpour P, Raj M, Kast J, Duronio V (2005) A proteolytic fragment of Mcl-1 exhibits nuclear localization and regulates cell growth by interaction with Cdk1. Biochem J 387:659-667.

Kenney AM, Cole MD, Rowitch DH (2003) Nmyc upregulation by sonic hedgehog signaling promotes proliferation in developing cerebellar granule neuron precursors. Development 130:15-28.

Kerr JF, Wyllie AH, Currie AR (1972) Apoptosis: a basic biological phenomenon with wide-ranging implications in tissue kinetics. Br J Cancer 26:239-257.

King RW, Jackson PK, Kirschner MW (1994) Mitosis in transition. Cell 79:563-571.

Kiyokawa H, Kineman RD, Manova-Todorova KO, Soares VC, Hoffman ES, Ono M, Khanam D, Hayday AC, Frohman LA, Koff A (1996) Enhanced growth of mice lacking the cyclin-dependent kinase inhibitor function of p27(Kip1). Cell 85:721-732.

Knudson CM, Johnson GM, Lin Y, Korsmeyer SJ (2001) Bax accelerates tumorigenesis in p53-deficient mice. Cancer Res 61:659-665.

Kozopas KM, Yang T, Buchan HL, Zhou P, Craig RW (1993) MCL1, a gene expressed in programmed myeloid cell differentiation, has sequence similarity to BCL2. Proc Natl Acad Sci U S A 90:3516-3520.

Krajewska M, Mai JK, Zapata JM, Ashwell KW, Schendel SL, Reed JC, Krajewski S (2002) Dynamics of expression of apoptosis-regulatory proteins Bid, Bcl-2, Bcl-X, Bax and Bak during development of murine nervous system. Cell Death Differ 9:145-157.

Kriegstein AR, Gotz M (2003) Radial glia diversity: a matter of cell fate. Glia 43:37-43.

Kuida K, Haydar TF, Kuan CY, Gu Y, Taya C, Karasuyama H, Su MS, Rakic P, Flavell RA (1998) Reduced apoptosis and cytochrome c-mediated caspase activation in mice lacking caspase 9. Cell 94:325-337.

Kwon HJ, Ma S, Huang Z (2011) Radial glia regulate Cajal-Retzius cell positioning in the early embryonic cerebral cortex. Dev Biol 351:25-34.

Lee WH, Bookstein R, Hong F, Young LJ, Shew JY, Lee EY (1987) Human retinoblastoma susceptibility gene: cloning, identification, and sequence. Science 235:1394-1399.

Leonard JR, D'Sa C, Cahn BR, Korsmeyer SJ, Roth KA (2001) Bid regulation of neuronal apoptosis. Brain Res Dev Brain Res 128:187-190.

Leone DP, Srinivasan K, Chen B, Alcamo E, McConnell SK (2008) The determination of projection neuron identity in the developing cerebral cortex. Curr Opin Neurobiol 18:28-35.

Liu W, Staecker H, Stupak H, Malgrange B, Lefebvre P, Van De Water TR (1998) Caspase inhibitors prevent cisplatin-induced apoptosis of auditory sensory cells. Neuroreport 9:2609-2614.

Loda M, Cukor B, Tam SW, Lavin P, Fiorentino M, Draetta GF, Jessup JM, Pagano M (1997) Increased proteasome-dependent degradation of the cyclin-dependent kinase inhibitor p27 in aggressive colorectal carcinomas. Nat Med 3:231-234.

Malatesta P, Appolloni I, Calzolari F (2008) Radial glia and neural stem cells. Cell Tissue Res 331:165-178.

Malumbres M, Barbacid M (2009) Cell cycle, CDKs and cancer: a changing paradigm. Nat Rev Cancer 9:153-166.

Martin A, Odajima J, Hunt SL, Dubus P, Ortega S, Malumbres M, Barbacid M (2005) Cdk2 is dispensable for cell cycle inhibition and tumor suppression mediated by p27(Kip1) and p21(Cip1). Cancer Cell 7:591-598.

Martinez-Cerdeno V, Noctor SC, Kriegstein AR (2006) The role of intermediate progenitor cells in the evolutionary expansion of the cerebral cortex. Cereb Cortex 16 Suppl 1:i152-161.

Martinou JC, Dubois-Dauphin M, Staple JK, Rodriguez I, Frankowski H, Missotten M, Albertini P, Talabot D, Catsicas S, Pietra C, et al. (1994) Overexpression of BCL-2 in transgenic mice protects neurons from naturally occurring cell death and experimental ischemia. Neuron 13:1017-1030.

McConnell SK (1995) Constructing the cerebral cortex: neurogenesis and fate determination. Neuron 15:761-768.

Megason SG, McMahon AP (2002) A mitogen gradient of dorsal midline Wnts organizes growth in the CNS. Development 129:2087-2098.

Merkle FT, Alvarez-Buylla A (2006) Neural stem cells in mammalian development. Curr Opin Cell Biol 18:704-709.

Michaelidis TM, Sendtner M, Cooper JD, Airaksinen MS, Holtmann B, Meyer M, Thoenen H (1996) Inactivation of bcl-2 results in progressive degeneration of motoneurons, sympathetic and sensory neurons during early postnatal development. Neuron 17:75-89.

Miyata T, Kawaguchi A, Saito K, Kawano M, Muto T, Ogawa M (2004) Asymmetric production of surface-dividing and non-surface-dividing cortical progenitor cells. Development 131:3133-3145.

Molyneaux BJ, Arlotta P, Menezes JR, Macklis JD (2007) Neuronal subtype specification in the cerebral cortex. Nat Rev Neurosci 8:427-437.

Montagnoli A, Fiore F, Eytan E, Carrano AC, Draetta GF, Hershko A, Pagano M (1999) Ubiquitination of p27 is regulated by Cdk-dependent phosphorylation and trimeric complex formation. Genes Dev 13:1181-1189.

Motoyama N, Wang F, Roth KA, Sawa H, Nakayama K, Negishi I, Senju S, Zhang Q, Fujii S, et al. (1995) Massive cell death of immature hematopoietic cells and neurons in Bcl-x-deficient mice. Science 267:1506-1510.

Musgrove EA, Davison EA, Ormandy CJ (2004) Role of the CDK inhibitor p27 (Kip1) in mammary development and carcinogenesis: insights from knockout mice. J Mammary Gland Biol Neoplasia 9:55-66.

Nakayama K, Ishida N, Shirane M, Inomata A, Inoue T, Shishido N, Horii I, Loh DY (1996) Mice lacking p27(Kip1) display increased body size, multiple organ hyperplasia, retinal dysplasia, and pituitary tumors. Cell 85:707-720.

Nevins JR (1998) Toward an understanding of the functional complexity of the E2F and retinoblastoma families. Cell Growth Differ 9:585-593.

Nguyen L, Besson A, Heng JI, Schuurmans C, Teboul L, Parras C, Philpott A, Roberts JM, Guillemot F (2006) p27kip1 independently promotes neuronal differentiation and migration in the cerebral cortex. Genes Dev 20:1511-1524.

Nicholson DW, Ali A, Thornberry NA, Vaillancourt JP, Ding CK, Gallant M, Gareau Y, Griffin PR, Labelle M, Lazebnik YA, et al. (1995) Identification and inhibition of the ICE/CED-3 protease necessary for mammalian apoptosis. Nature 376:37-43.

Nieto M, Monuki ES, Tang H, Imitola J, Haubst N, Khoury SJ, Cunningham J, Gotz M, Walsh CA (2004) Expression of Cux-1 and Cux-2 in the subventricular zone and upper layers II-IV of the cerebral cortex. J Comp Neurol 479:168-180.

Nigg EA (1995) Cyclin-dependent protein kinases: key regulators of the eukaryotic cell cycle. Bioessays 17:471-480.

Noctor SC, Martinez-Cerdeno V, Ivic L, Kriegstein AR (2004) Cortical neurons arise in symmetric and asymmetric division zones and migrate through specific phases. Nat Neurosci 7:136-144.

Nurse P (1994) Ordering S phase and M phase in the cell cycle. Cell 79:547-550.

Ohtsubo M, Theodoras AM, Schumacher J, Roberts JM, Pagano M (1995) Human cyclin E, a nuclear protein essential for the G1-to-S phase transition. Mol Cell Biol 15:2612-2624.

Opferman JT, Iwasaki H, Ong CC, Suh H, Mizuno S, Akashi K, Korsmeyer SJ (2005) Obligate role of anti-apoptotic MCL-1 in the survival of hematopoietic stem cells. Science 307:1101-1104.

Orike N, Middleton G, Borthwick E, Buchman V, Cowen T, Davies AM (2001) Role of PI 3-kinase, Akt and Bcl-2-related proteins in sustaining the survival of neurotrophic factor-independent adult sympathetic neurons. J Cell Biol 154:995-1005.

Pagano M, Tam SW, Theodoras AM, Beer-Romero P, Del Sal G, Chau V, Yew PR, Draetta GF, Rolfe M (1995) Role of the ubiquitin-proteasome pathway in regulating abundance of the cyclin-dependent kinase inhibitor p27. Science 269:682-685.

Pardee AB (1989) G1 events and regulation of cell proliferation. Science 246:603-608.

Parent JM (2003) Injury-induced neurogenesis in the adult mammalian brain. Neuroscientist 9:261-272.

Polager S, Ginsberg D (2008) E2F - at the crossroads of life and death. Trends Cell Biol 18:528-535.

Rakic P (1988) Specification of cerebral cortical areas. Science 241:170-176.

Reynolds BA, Weiss S (1992) Generation of neurons and astrocytes from isolated cells of the adult mammalian central nervous system. Science 255:1707-1710.

Rinkenberger JL, Horning S, Klocke B, Roth K, Korsmeyer SJ (2000) Mcl-1 deficiency results in peri-implantation embryonic lethality. Genes Dev 14:23-27.

Roth KA, Kuan C, Haydar TF, D'Sa-Eipper C, Shindler KS, Zheng TS, Kuida K, Flavell RA, Rakic P (2000) Epistatic and independent functions of caspase-3 and Bcl-X(L) in developmental programmed cell death. Proc Natl Acad Sci U S A 97:466-471.

Roussel MF (1998) Key effectors of signal transduction and G1 progression. Adv Cancer Res 74:1-24.

Santamaria D, Barriere C, Cerqueira A, Hunt S, Tardy C, Newton K, Caceres JF, Dubus P, Malumbres M, Barbacid M (2007) Cdk1 is sufficient to drive the mammalian cell cycle. Nature 448:811-815.

Sauer B (1998) Inducible gene targeting in mice using the Cre/lox system. Methods 14:381-392.

Savitt JM, Jang SS, Mu W, Dawson VL, Dawson TM (2005) Bcl-x is required for proper development of the mouse substantia nigra. J Neurosci 25:6721-6728.

Schwickart M, Huang X, Lill JR, Liu J, Ferrando R, French DM, Maecker H, O'Rourke K, Bazan F, Eastham-Anderson J, Yue P, Dornan D, Huang DC, Dixit VM (2010) Deubiquitinase USP9X stabilizes MCL1 and promotes tumour cell survival. Nature 463:103-107.

Sherr CJ (1994) The ins and outs of RB: coupling gene expression to the cell cycle clock. Trends Cell Biol 4:15-18.

Sherr CJ (1995) D-type cyclins. Trends Biochem Sci 20:187-190.

Sitailo LA, Jerome-Morais A, Denning MF (2009) Mcl-1 functions as major epidermal survival protein required for proper keratinocyte differentiation. J Invest Dermatol 129:1351-1360.

Sjostrom SK, Finn G, Hahn WC, Rowitch DH, Kenney AM (2005) The Cdk1 complex plays a prime role in regulating N-myc phosphorylation and turnover in neural precursors. Dev Cell 9:327-338.

Sosunov AA, Chelyshev Iu A (2002) [Neural stem cells in the brain]. Usp Fiziol Nauk 33:17-28.

Takahashi H, Liu FC (2006) Genetic patterning of the mammalian telencephalon by morphogenetic molecules and transcription factors. Birth Defects Res C Embryo Today 78:256-266.

Takahashi T, Nowakowski RS, Caviness VS, Jr. (1996) Interkinetic and migratory behavior of a cohort of neocortical neurons arising in the early embryonic murine cerebral wall. J Neurosci 16:5762-5776.

Tarui T, Takahashi T, Nowakowski RS, Hayes NL, Bhide PG, Caviness VS (2005) Overexpression of p27 Kip 1, probability of cell cycle exit, and laminar destination of neocortical neurons. Cereb Cortex 15:1343-1355.

Taylor RC, Cullen SP, Martin SJ (2008) Apoptosis: controlled demolition at the cellular level. Nat Rev Mol Cell Biol 9:231-241.

Tropepe V, Sibilia M, Ciruna BG, Rossant J, Wagner EF, van der Kooy D (1999) Distinct neural stem cells proliferate in response to EGF and FGF in the developing mouse telencephalon. Dev Biol 208:166-188.

Vairo G, Soos TJ, Upton TM, Zalvide J, DeCaprio JA, Ewen ME, Koff A, Adams JM (2000) Bcl-2 retards cell cycle entry through p27(Kip1), pRB relative p130, and altered E2F regulation. Mol Cell Biol 20:4745-4753.

Vanderluit JL, Ferguson KL, Nikoletopoulou V, Parker M, Ruzhynsky V, Alexson T, McNamara SM, Park DS, Rudnicki M, Slack RS (2004) p107 regulates neural precursor cells in the mammalian brain. J Cell Biol 166:853-863.

Vanderluit JL, Wylie CA, McClellan KA, Ghanem N, Fortin A, Callaghan S, MacLaurin JG, Park DS, Slack RS (2007) The Retinoblastoma family member p107 regulates the rate of progenitor commitment to a neuronal fate. J Cell Biol 178:129-139.

Vick B, Weber A, Urbanik T, Maass T, Teufel A, Krammer PH, Opferman JT, Schuchmann M, Galle PR, Schulze-Bergkamen H (2009) Knockout of myeloid cell leukemia-1 induces liver damage and increases apoptosis susceptibility of murine hepatocytes. Hepatology 49:627-636.

Wang JM, Chao JR, Chen W, Kuo ML, Yen JJ, Yang-Yen HF (1999) The antiapoptotic gene mcl-1 is up-regulated by the phosphatidylinositol 3-kinase/Akt signaling pathway through a transcription factor complex containing CREB. Mol Cell Biol 19:6195-6206.

Wang JM, Lai MZ, Yang-Yen HF (2003) Interleukin-3 stimulation of mcl-1 gene transcription involves activation of the PU.1 transcription factor through a p38 mitogen-activated protein kinase-dependent pathway. Mol Cell Biol 23:1896-1909.

Wang ZB, Liu YQ, Cui YF (2005) Pathways to caspase activation. Cell Biol Int 29:489-496.

Warr MR, Acoca S, Liu Z, Germain M, Watson M, Blanchette M, Wing SS, Shore GC (2005) BH3-ligand regulates access of MCL-1 to its E3 ligase. FEBS Lett 579:5603-5608.

Warr MR, Shore GC (2008) Unique biology of Mcl-1: therapeutic opportunities in cancer. Curr Mol Med 8:138-147.

Weber A, Boger R, Vick B, Urbanik T, Haybaeck J, Zoller S, Teufel A, Krammer PH, Opferman JT, Galle PR, Schuchmann M, Heikenwalder M, Schulze-Bergkamen H (2010) Hepatocyte-specific deletion of the antiapoptotic protein myeloid cell leukemia-1 triggers proliferation and hepatocarcinogenesis in mice. Hepatology 51:1226-1236.

Weinberg RA (1995) The retinoblastoma protein and cell cycle control. Cell 81:323-330.

White FA, Keller-Peck CR, Knudson CM, Korsmeyer SJ, Snider WD (1998) Widespread elimination of naturally occurring neuronal death in Bax-deficient mice. J Neurosci 18:1428-1439.

Youle RJ, Strasser A (2008) The BCL-2 protein family: opposing activities that mediate cell death. Nat Rev Mol Cell Biol 9:47-59.

Zheng YL, Li BS, Rudrabhatla P, Shukla V, Amin ND, Maric D, Kesavapany S, Kanungo J, Pareek TK, Takahashi S, Grant P, Kulkarni AB, Pant HC (2010) Phosphorylation of p27Kip1 at Thr187 by cyclin-dependent kinase 5 modulates neural stem cell differentiation. Mol Biol Cell 21:3601-3614.

Zhong Q, Gao W, Du F, Wang X (2005) Mule/ARF-BP1, a BH3-only E3 ubiquitin ligase, catalyzes the polyubiquitination of Mcl-1 and regulates apoptosis. Cell 121:1085-1095.

Zhong W, Chia W (2008) Neurogenesis and asymmetric cell division. Curr Opin Neurobiol 18:4-11.

Zhu Y, Yang GY, Ahlemeyer B, Pang L, Che XM, Culmsee C, Klumpp S, Krieglstein J (2002) Transforming growth factor-beta 1 increases bad phosphorylation and protects neurons against damage. J Neurosci 22:3898-3909.

Zindy F, Cunningham JJ, Sherr CJ, Jogal S, Smeyne RJ, Roussel MF (1999) Postnatal neuronal proliferation in mice lacking Ink4d and Kip1 inhibitors of cyclin-dependent kinases. Proc Natl Acad Sci U S A 96:13462-13467.

Zinkel S, Gross A, Yang E (2006) BCL2 family in DNA damage and cell cycle control. Cell Death Differ 13:1351-1359.